MASS. INST. OF TECHNOLOGY
APR 24 1968
LIBRARIES

# A WIDE DYNAMIC RANGE SINGLE-SIDEBAND RECEIVER

by

MICHAEL JOHN WARD

S.B., Massachusetts Institute
of Technology
(1966)

SUBMITTED IN PARTIAL FULFILLMENT OF THE

REQUIREMENTS FOR THE DEGREE OF

MASTER OF SCIENCE

at the

MASSACHUSETTS INSTITUTE OF TECHNOLOGY
December, 1967

Signature of Author _____
Department of Electrical Engineering, December 22, 1967

Certified by _____
Thesis Supervisor

Accepted by _____
Chairman, Departmental Committee on Graduate Students

A WIDE DYNAMIC RANGE SINGLE-SIDEBAND RECEIVER

by

MICHAEL JOHN WARD

Submitted to the Department of Electrical Engineering on December 22, 1967, in partial fulfillment of the requirements for the Degree of Master of Science

ABSTRACT

A receiver should have a wide dynamic range to reduce spurious responses to internally generated intermodulation distortion. The mathematics of an unusual four-FET mixer are developed, and compared with the conversion properties and intermodulation limitations of the simple nonlinear-resistor mixer.

The effects of frequency-dependent terminations on the input and output are discussed, and found to be highly important to operation as a mixer. Departures from the ideal case are analyzed, and their effects modeled as external perturbations on the ideal mixer. Expressions for the mixer conversion loss and sensitivity, and relative generated intermodulation power are developed, completely describing the dynamic range in terms of measureable device parasitic impedances.

The experimental section describes the methods used to measure the various mixer and receiver parameters, and gives probable error ranges. The mixer receiver is found to have a transducer conversion loss of 7 db, with a signal sensitivity of -120 dbm for a 10 db [S+N]/N in a 1 KHz bandwidth. This is compared with the values found for the laboratory receiver, a Collins R-390, with the same sensitivity. The dynamic range of the mixer is found to be 120 db $\pm$ 5 db, as compared with 83 db for the R-390.

The degenerate behavior of the IM level at high drive levels is discussed as an inquiry into the $\pm$5 db uncertainty in dynamic range. The individual device characteristics are measured and values of sensitivity and dynamic range are calculated using expressions developed earlier; they are found to be identical to within the limit of experimental error.

In appendices the theory of intermodulation is developed in more detail. The normal assumptions of IM generation are found to be insufficient, and the two-pass analysis of IM is developed. An expression for the total third-order IM power at the IF frequency is derived. Further appendices explore methods of IM generation in purely square-law mixers and the possible intermodulation-free cube-law mixer.

THESIS SUPERVISOR: Robert P. Rafuse
TITLE: Associate Professor of Electrical Engineering

## ACKNOWLEDGMENT

The author wishes to express his deepest thanks to Professor Robert P. Rafuse, without whose continual help and guidance this thesis would not have existed in any sense.

Thanks are also due Dr. Donald H. Steinbrecher for his ability to lay bare the essentials of a problem and his help in organization.

Final thanks are due the Research Laboratory of Electronics for the experimental support.

TABLE OF CONTENTS


| | Page |
|---|---|
| Introduction | 6 |
| Receiver Operation: | 6 |
| Functional Description of a Typical Receiver | 6 |
| Frequency Conversion and Mixer Operation Nonlinear Resistance | 9 |
| The Balanced-Bridge Switching-State Mixer | 16 |
| Ideal Case Analysis | 16 |
| Device Limitations | 23 |
| Parasitic Impedance Analysis | 23 |
| Conversion Loss | 32 |
| Signal Level Perturbations | 33 |
| Transition-Time Behavior | 35 |
| Summary of Theoretical Analysis | 35 |
| Experimental | 39 |
| Organization and Equipment | 39 |
| Discussion of Subunits | 43 |
| Mixer | 43 |
| Crystal Filters | 43 |
| IF Amplifier | 46 |
| Low-Pass Filter | 49 |
| Diplexer | 49 |
| Phase Detector | 49 |
| Second Local Oscillator | 53 |
| Power Amplifier and First Local Oscillator | 55 |

| | Page |
|---|---|
| Experimental Results | 57 |
| Receiver Performance and Dynamic Range | 57 |
| Sensitivity and Conversion Loss | 61 |
| Intermodulation Generated in Odd-Order Off-State Reverse Transconductances | 62 |
| Conclusions | 67 |
| Footnotes | 69 |
| Bibliography | 70 |
| Appendices | 71 |
| Intermodulation | 71 |
| Intermodulation in Perfect Square-Law Devices | 78 |

# A WIDE DYNAMIC RANGE SINGLE-SIDEBAND RECEIVER

## INTRODUCTION

The ability of a communications link to transmit information is limited by several factors. These include the transmitted power and receiver sensitivity to signal power, versus the system noise level and path loss. Also important is the system bandwidth required--the rate and type of modulation, compared with the bandwidth available. A final consideration is the system susceptibility to or freedom from spurious responses, whether caused by intentional jamming of the desired signals, or by accidental overload of the receiver. This thesis involves the design and experimental development of a receiver, for undesignated general use in the HF region (3 to 30 MHz), which is largely free of undesired responses and spurious signals created by intermodulation distortion. The receiver obtains the necessary sensitivity, bandwidth, and modulation detection capabilities congruent with its high dynamic range, through the use of an unusual mixer based on a bridge of four Metal Oxide-Semiconductor Field-Effect Transistors (MOSFET) and following stages designed for high dynamic range with low noise.

## FUNCTIONAL DESCRIPTION OF A TYPICAL RECEIVER

The basic function of a receiver is to convert a radio-frequency signal onto which some information has been impressed into some other signal in which form the information is readily accessible. With a radiotelephone

signal, for example, the desired output would be an audio-frequency (AF) signal driving a speaker or line; with radioteletype, on the other hand, a digital output is required to drive a local or remote teleprinter. A typical superheterodyne receiver for radiotelephone signals might have a block diagram similar to Fig. (1).

With the normal range of received signal voltages ($10^{-6}$V to 1.0V) it is necessary to provide signal amplification before the information can be processed. The basic superheterodyne provides most of this amplification at the intermediate frequency (IF) with the AF amplifier designed primatily to drive the output device. The function of the mixer or frequency converter then becomes the raising or lowering of the received signal frequency to the IF frequency. The local oscillator may be embedded in the mixer; it is shown here separately for clarity. The detector or demodulator processes the IF signal to make the information available for distribution by the output device; it also specifies the modulation forms which can be received.

The signal sensitivity of this simple receiver is fixed by the noise figure of the IF amplifier, the conversion loss of the mixer, and the insertion losses of whatever impedance matching networks may exist between the mixer and the IF stages. Although the selectivity function (bandwidth determining devices) may be placed anywhere in the circuit, there are certain advantages in placing them between the mixer and the IF amplifier. The dynamic range of this receiver is set by the entire system; if there is zero conversion loss, from RF to output, each "black box" must have the same dynamic range. Placing the selective circuits directly after the mixer, however, eliminates the effects of out-of-band signals on the IF amplifier and following stages, and, at least for the intermodulation measure of dynamic range, reduces the

FIG. 1

required range of the following stages by the amount in decibels of the selective attenuation of out-of-band signals.

Throughout this thesis dynamic range (DR) will be used as a measure of system susceptibility to intermodulation distortion (IM). For this receiving system the sensitivity is defined as the smallest signal which will produce an output signal ten decibels (10 db) above the output noise level for a specified bandwidth (usually 1 KHz). A high-level two-tone signal, with frequencies chosen such that $2\omega_1 \pm \omega_2 = \omega_{sig}$, is introduced at a power level sufficient to produce third-order IM products 10 db above the noise level. The total dynamic range is then $P_{two\text{-}tone} - P_{signal}$ (in db). The dynamic range of the system can be extended by increasing system sensitivity (limited only by the thermal noise level--i.e. a noise figure of 0 db is the best possible) and by increasing the power levels at which the internal components will operate without "nonlinear" behavior. Although both methods are used for increasing the DR of the receiver described in this thesis, the major effort has been in designing mixers and following stages resistant to high power levels.

## FREQUENCY CONVERSION AND MIXER OPERATION

### NONLINEAR RESISTANCE

The function of the mixer is to add or subtract a locally generated RF signal frequency to the frequency of the desired input signal in such a way that the output is a signal at the IF frequency. Ideally the mixer has zero conversion loss and $P_{IF}=P_{RF}$. The simplest mixer is a nonlinear resistance with proper frequency-dependent networks attached. It is worth while describing such a mixer in some detail; although the mixer used in this thesis is quite different in principles of operation, the fundamental limitations on its

dynamic range can be estimated by modeling its departures from the ideal model as parasitic nonlinear-resistance mixers.

Any nonlinear device (one in which the transfer function is a function of the value of one of the input variables) may be represented as a power series around some point value. For example, we may define the value of a nonlinear resistor as a power series in I, the instantaneous current through the resistor:

$$R(I) = r_o + r_1 I + r_2 I^2 + r_3 I^3 + \cdots + r_n I^n \qquad (1)$$

Then the voltage across the resistor is (Fig. (2a) )

$$V = IR(I) = r_o I + r_1 I^2 + r_2 I^3 + \cdots + r_n I^{n+1} \qquad (2)$$

Assume the series can be terminated with little error at the second term:

$$V = r_o I + r_1 I^2 \qquad (3)$$

Suppose the current consists of two sinusoidal currents, $I_1$ and $I_2$, at frequencies $\omega_1$ and $\omega_2$. Then the output voltage

$$V = r_o(I_1 \cos\omega_1 t + I_2 \cos\omega_2 t) + r_1(I_1 \cos\omega_1 t + I_2 \cos\omega_2 t)^2 \qquad (4)$$

The linear term simply reproduces the input signal. The square term, however, gives:

$$V_{sq} = r_1( I_1^2 \cos^2\omega_1 t + 2 I_1 I_2 \cos\omega_1 t \cos\omega_2 t + I_2^2 \cos^2\omega_2 t ) \qquad (5)$$

recalling from trigonometry $\cos^2 x = (1 + \cos 2x)/2$ (6)

and $\cos x \cos y = \frac{1}{2}[ \cos(x+y) + \cos(x-y) ]$ (7)

it becomes clear that the $V_{sq}$ term gives output signals at the frequencies $2\omega_1$ and $2\omega_2$, DC, and $\omega_1+\omega_2$ and $\omega_1-\omega_2$. If we define $\omega_1$ as the signal frequency, and $\omega_2$ as the local oscillator frequency, such that $\pm(\omega_2-\omega_1) = \omega_{IF}$, the square law nonlinear resistor can be used as a frequency converter. (Note that the converter will also respond to a signal at the image frequency $\omega_r$, chosen such that $\omega_r = \omega_{LO} + \omega_{IF}$; a signal at this frequency will combine with the LO signal

to produce output frequencies of the form $\pm\omega_r \pm \omega_{LO}$, and the difference product is also equal to the IF frequency. The normal procedure in mixer design is to short circuit or open circuit the image frequency at the input with frequency selective circuitry, simply to eliminate the power at this frequency at the input port.[1] This is not always possible; in the mixer which will be described later, the exact form of the image termination becomes highly important. For the purposes of this discussion, however, it is assumed that the image response is eliminated thaough some unspecified means.)

At the output port,

$$V_{IF} = r_1(I_{sig} I_{LO})\cos\omega_{IF} t \qquad (8)$$

The assumption has been made that the resistor can be described adequately be a linear term and a square-law term. In practice this is not valid over an infinite range, and at some power level the cubic term of the power series expansion begins to contribute measureable output power:

$$V_{cubic} = r_2(I_1\cos\omega_1 t + I_2\cos\omega_2 t)^3 \qquad (9)$$

$$V_{cu.} = r_2(\ I_1^3\cos^3\omega_1 t + 3I_1^2 I_2\cos^2\omega_1 t\cos\omega_2 t + 3I_1 I_2^2\cos\omega_1 t\cos\omega_2 t + I_2^3\cos^3\omega_2 t) \qquad (10)$$

The cubic term, when expanded, contains frequency components at $\omega_1$ and $\omega_2$, at $3\omega_1$ and $3\omega_2$ and at $2\omega_1 \pm \omega_2$ and $2\omega_2 \pm \omega_1$. These terms at frequencies of the form $2\omega_i \pm \omega_j$ are the third-order intermodulation (IM) terms, spurious responses generated by the mixer at an output frequency different from the input frequencies. The danger occurs when one of the third order sums or differences falls near the desired signal; in this case the receiver will amplify, demodulate, and output this internally generated spurious signal as if it were present at the input.

The actual mechanism for generation of third order IM is a bit more complex than appears from the foregoing discussion. For a more complete analysis

see Appendix I; however, a few lines can indicate the process of IM generation. Assume the input port sees the local oscillator at $\omega_{LO}$, and two undesired signals at $\omega_3$ and $\omega_4$. Further assume that the desired signal is at a frequency $\omega_{sig} = \omega_{LO} - \omega_{IF}$ and that the undesired signals occur such that $2\omega_3 - \omega_4 = \omega_s$. (See Fig.(2b), which has $\omega_3$ and $\omega_4$ slightly offset to show their frequencies and the frequencies of their third-order products.) This is the normal situation with third-order IM; if the $\omega_{IF}$ = (30MHz) (suppressing the $2\pi$ factors for ease in writing--a "shorthand") and $\omega_s$ = 10 MHz (values taken from the experimental portion of the thesis) then the third order term will satisfy the above relations for $\omega_3$=12MHz and $\omega_4$=14MHz, or $\omega_3$=15MHz and $\omega_4$=20MHz, or any other combination such that $2\omega_3 - \omega_4 = \omega_s$. The cubic term will produce a voltage at the third-order difference frequency, $2\omega_3 - \omega_4$, but this voltage must still be converted down to the IF frequency by the square-law portion of the device. In short, any IM production mechanisms must occur separately from the conversion mechanism, and third-order IM is generated by signals going through the mixer twice--once to generate the odd-order term, and once to convert the odd-order term to the IF frequency.

To illustrate, let the resistor power series expansion be divided into odd and even functions of I: $R(I) = R_o(I) + R_e(I)$ (11)

Then the current is common to both the odd and even parts of the resistance, and the voltage may be divided into odd and even functions:

$$V = V_o + V_e \tag{12}$$

where $V_o = IR_e(I)$ (13a) and $V_e = IR_o(I)$ (13b)

The cubic term shows up in $V_o$:

$$V_{cubic} = (3/4) r_2 I_3^2 I_4 \cos(2\omega_3 - \omega_4)t \tag{14}$$

This is transmitted through the externam networds as an odd-order current into the even-order resistance terms; if we let the transmission constant be K, then

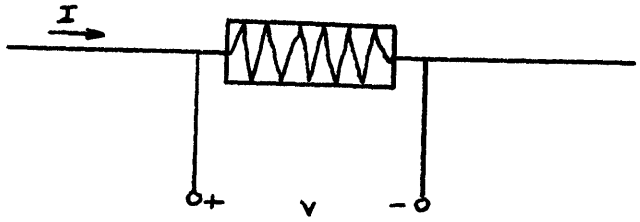


FIG. 2a

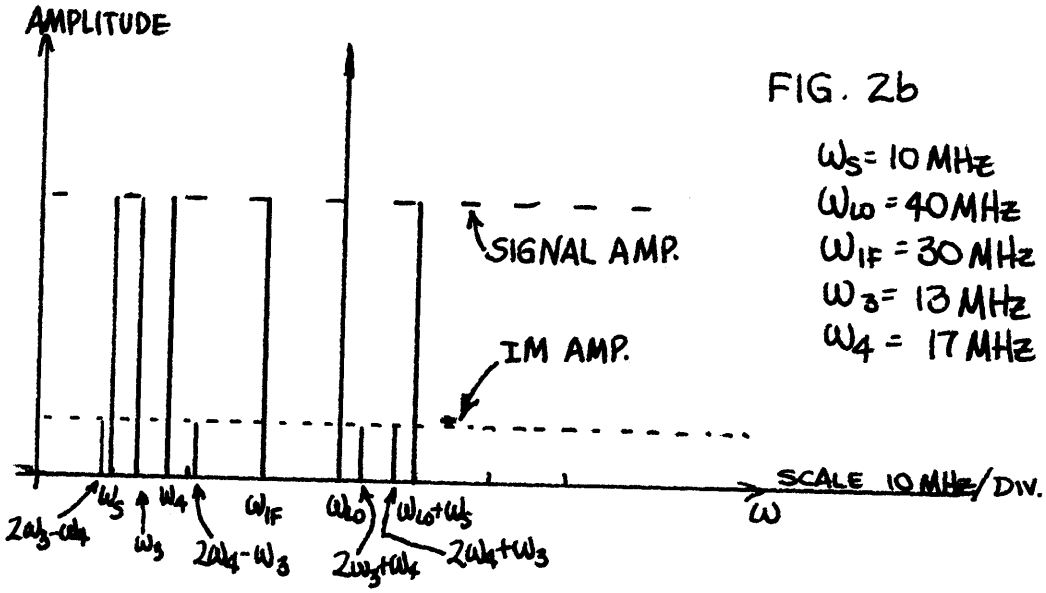


FIG. 2b

$\omega_S = 10$ MHz
$\omega_{LO} = 40$ MHz
$\omega_{IF} = 30$ MHz
$\omega_3 = 13$ MHz
$\omega_4 = 17$ MHz

the final intermodulation voltage

$$V_{IM} = (3/4)Kr_1r_2I_3^2I_4I_{LO}\cos\omega_{IF}t \tag{15}$$

If it is assumed that both the signal power (converted to the IF) and the IM power (also at the IF) have the same load (since they are at the same frequency), the dynamic range, as defined as the range between some arbitrary signal power and the number of decibels lower in power the IM signal is,

$$D.R. = \frac{P_{gen.by\ signal}}{P_{gen.by\ IM}} = \frac{\left|V_{IF(sig)}\right|^2}{\left|V_{IF(IM)}\right|^2} = \frac{\left|(r_1\ \ )I_sI_{LO}\right|^2}{\left|(3/4)Kr_1r_2I_3^2I_4I_{LO}\right|^2} \tag{16}$$

(Note that this measure of dynamic range may be related to the usual measure by setting IM power level at 10 db above the noise level. Then the output signal power will be greater than the IM power by the amount (in decibels) of the dynamic range.)

Assume equal signal power and undesired signal powers--$I_s = I_3 = I_4 = I$

$$D.\ R. = \frac{1}{\frac{9}{16}K^2r_2^2\ I^4} \tag{17}$$

Note that since $r_1$ has units of volts/cur$^2$ and $r_2$ has units of volts/cur$^3$ the K has units of cur/volts and the dynamic range is dimensionless, as expected. Since we have assumed equal signal powers, the IM signal has twice the total power, in its two-tone, of the desired signal; hence the total dynamic range calculated above will be twice as great (+3 db) as the range measured according to the 10 db above the noise criteria defined on a previous page. For measurements with equal powers, therefore, 3 db must be added to the experimental result to denote actual dynamic range.

Examining the above expression for dynamic range, it becomes clear that intermodulation may be reduced (D. R. increased) by lowering the coefficient

of the cubic term (as expected) and by reducing the coupling coeffient that allows the third-order terms to feed into the even-order (square-law) frequency conversion portion.

An interesting feature of this mixer is that without the square-law conversion term, no IM will be generated. If some way were found to generate second-order sums and differences without a square-law term, the mixer would have an indefinite dynamic range. (More properly, if a mixer could be developed with no even-order terms, no IM could be generated.) The pure square-law mixer is normally considered to have this characteristic, but this is not necessarily true, depending on the terminations of the second-harmonic components. (See Appendix II). If a mixer having a purely cube-law characteristic is fed with the signal and LO frequencies and a DC offset voltage (a voltage at the frequency $\omega_{DC} = 0$) the output will produce frequencies of the form $\cos(0 \pm \omega_{LO} \pm \omega_s)t = \cos\omega_{IF}t$ and frequency conversion will take place. The limitation on this scheme is that all higher order terms in the polynomial expansion will produce IM, both the odd-order terms and the even-order terms.

## THE BALANCED-BRIDGE SWITCHING-STATE MIXER

The method of operation of the balanced-bridge mixer is fundamentally different from the nonlinear-resistance method of frequency conversion.[2,3,4] In its simplest form, it requires four devices with measureably different "on" and "off" states, with a means for externally switching between the two states. (Fig. 3) Opposite pairs of devices on the bridge are turned on and off at the local oscillator frequency, and the entire mixer may be modeled as a double-pole double-throw reversing switch changing state at the LO rate. The exact type of device is not important; in the ideal model case they can be diodes,[5] transistors, FETs, or any other two-state devices. (For example, a mechanical switch, motor-driven, is entirely feasible at lower frequencies.) In the ideal-model case, the transfer characteristics of the individual devices become unimportant. The choice of MOS FETs for the experimental version of this mixer was dictated by the unavoidable departures from ideal switching states, in which cases the device characteristics do become important.

The device switching characteristic must occupy both the first and third quadrants of its I-V plot. The FET has both first and third quadrant regions of normal operation (Fig. 4a) while the diode first quadrant behavior is collapsed into the vertical positive current line and the third quadrant behavior into the horizontal negative voltage line. (Fig. 4b) The individual devices may switch either voltage or current; the bridge configuration satisfies power conservation at either port.

As an illustration, assume devices $D_1$ and $D_2$, $D_3$ and $D_4$ are paired two-state current-control devices, controlled by the third terminals crossing in the center of the bridge. (Fig. 3) Then, with $D_1$ and $D_2$ off (passing zero

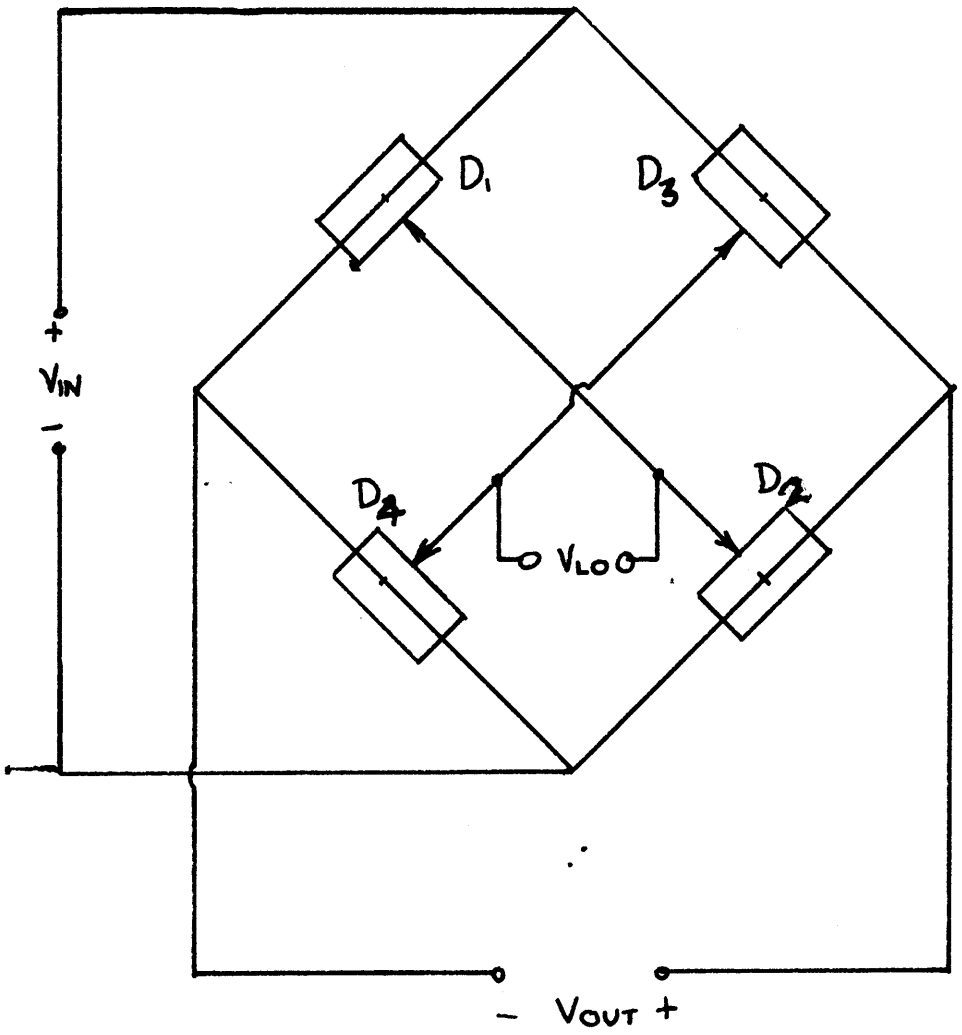


FIG. 3.

FIG. 4a.

IDEAL FET

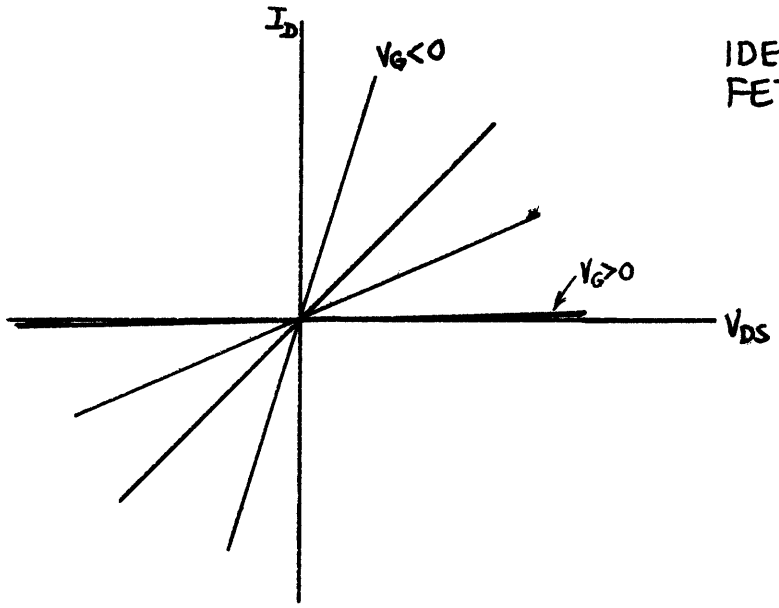


FIG. 4b.

IDEAL DIODE

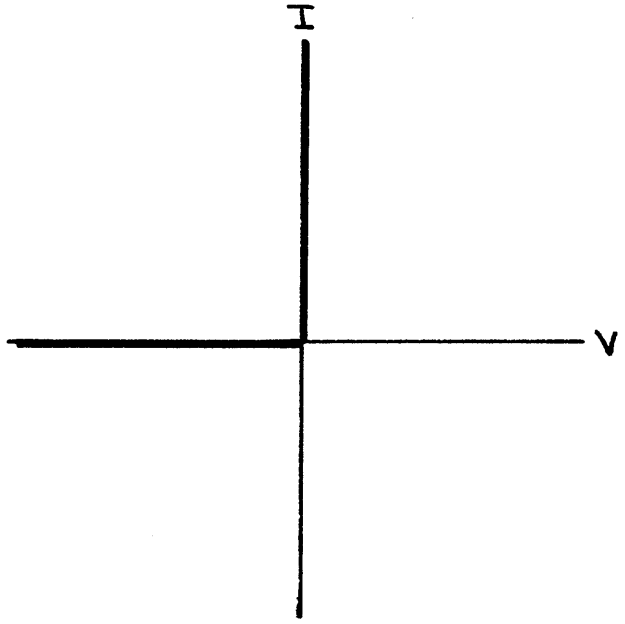

current) and $D_3$ and $D_4$ on, $I_{out} = I_{in}$ and $V_{out} = V_{in}$. With $D_1$ and $D_2$ on, and $D_3$ and $D_4$ off, $I_{out} = -I_{in}$ and $V_{out} = -V_{in}$. The ideal model, then, is the reversing switch.[6]

If the switch poles are driven at some switching rate $\epsilon(T)$, where $\epsilon(T)$ is a square wave reversing function (Fig. 5)

$$\epsilon(T) = \frac{2}{\pi} \sum_{n=\pm \text{odd}}^{\infty} \frac{e^{j\omega_{LO} nt}}{|n|} [-1]^{(|n|-1)/2} \tag{18}$$

it is possible to define an LO frequency $\omega_{LO} = 2\pi/T$ (Fig. 6).

If $V_{in} = V_s \cos\omega_s t$ then $V_{out} = V_{in}\epsilon(T)$ (19a)

$$V_{out} = V_s \frac{2}{\pi}[\cos(\omega_{LO}+\omega_s)t + \cos(\omega_{LO}-\omega_s)t] + \text{higher order terms} \tag{19b}$$

The higher order terms are all odd-order, of the form $m\omega_{LO} \pm \omega_s$ where m is even.

It should be noted at this point that frequency conversion has been achieved with nothing said about nonlinear resistance or individual device characteristics at all; the only assumption made was that both perfect switched states are attainable. For non-perfect switching the situation is more complicated, as will presently be shown; for the moment, however, attention will concentrated on evaluating the output signals and the effects of frequency dependent terminations.

Assuming a square wave switching waveform, the mixer can be modeled as a three-port (Fig. 6) not unlike the conventional mixer. The difference is that the black box has a simple time domain operation $\epsilon(T)$, corresponding to the frequency domain operation of mixing. At the IF (output) port,

$$V_{IF} = V_s \epsilon(T) \quad \text{and} \quad I_{IF} = I_s \epsilon(T) \tag{20}$$

Since $\epsilon(T)\cdot\epsilon(T)=1$, $V_s = V_{IF}\epsilon(T)$ and $I_s = I_{IF}\epsilon(T)$ (21)

and the mixer is bilateral--the output and input ports can be interchanged without affecting the conversion properties of the mixer.

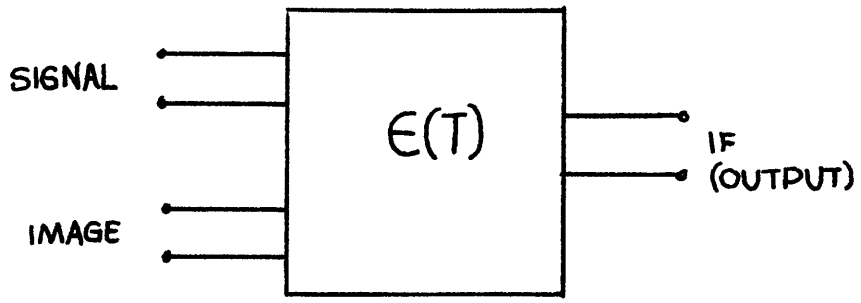


FIG. 6[redacted]

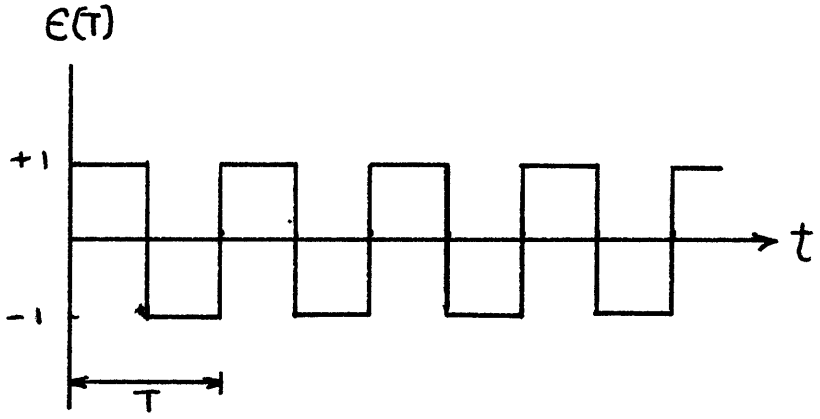


FIG [redacted] 5

Assuming a desired signal at $\omega_s$ is the only signal available at the input port, the output voltage

$$V_{OUT} = \frac{2}{\pi} V_s [\cos(\omega_{LO}-\omega_s)t + \cos(\omega_{LO}+\omega_s)t] \tag{22}$$

The output voltage has components at both the IF and sum frequencies,

$$V_{IF} = \frac{2}{\pi} [V_S + V^*_{SUM}] \tag{23}$$

It is possible to eliminate the sum frequency power at the output with a parallel-tuned LC trap set at the IF frequency; this sets $V^*_{SUM} = 0$ at the output, and

$$V_{IF} = \frac{2}{\pi} V_s \tag{24}$$

Since the mixer is completely bilateral, it is possible to look upon this IF voltage as an input signal at the reverse input port.

Then $V_s' = V_{IF}$ and the voltage at the input port

$$V_{reverse} = \frac{2}{\pi} V_{IF} [\cos(\omega_{LO}+\omega_{IF})t + \cos(\omega_{LO}-\omega_{IF})t] \tag{25}$$

This has components at the signal frequency and the image frequency, and

$$V_{S(rev.)} = \frac{2}{\pi} V_{IF} \quad \text{and} \quad V_{r(rev.)} = \frac{2}{\pi} V_{IF} \tag{26}$$

Hence $$V_{IF} = \frac{\pi}{2} V_{s(rev.)} = \frac{\pi}{2} V_{r(rev.)} \tag{27}$$

It is clear from Eqn. 27 that if the input appears as a short circuit at the image frequency, the IF output voltage drops to zero. The normal method of separating the signal and image ports and eliminating image response is to short circuit the image frequeicies at the input; this is clearly impossible here.

A similar analysis, performed for the current frequency components, shows that it is possible to terminate the currents independently of the voltages. The image frequency power may be eliminated at the input by open circuiting the input at the image frequency; the $I_{r(forward)}$ becomes zero and the $P_r$

also becomes zero. Thus we may eliminate image response by allowing no image frequency current to flow at the input, and eliminate sum frequency power by short circuiting the output for all but the IF frequency. Reversal of the input or output constraint--open circuiting the sum at the output instead of short circuiting it--requires reversing the other constraint. To summarize,

| | | |
|---|---|---|
| | If | sum frequency is shorted at output |
| | then | image frequency must be open circuited at input |
| OR: | If | sum frequency is open circuited at output |
| | then | image frequency must be shorted at input. |

The above equations show that shorting the signal frequency voltage or open circuiting its current will eliminate the IF frequency voltage or current at the output, which is not particularly surprising. Under short circuit sum--open circuit image constraints, the input impedance for some load resistance $R_L$ will be $\frac{4}{\pi^2} R_L$; the output current is $\frac{2}{\pi}$ times the signal current, since the apparent constraints are reversed for current. The total output power is $\frac{\pi}{2} V_{s\pi} \frac{2}{\pi} I_s = P_s$ and the mixer conversion loss is zero. With the constraints reversed for voltage, the input impedance is $\frac{\pi^2}{4} R_L$.

## DEVICE LIMITATIONS

It is unfortunately the case that no switching device is perfect. In general the "on" state will have a measureable voltage drop, and the "off" state a measureable current, due to parasitic impedances in series and parallel with the ideal switch model of each device. A second departure from perfection has to do with the switching waveform. It is apparent from the foregoing discussion that the optimum waveform is a simple square wave.[7] (This in itself is unusual, inasmuch as the single-ended mixer works best with a "conduction" waveform approaching an inpulse train.[7,8] The reversing switch model requires that equal time periods be spent in the "off" and "on" states for each device, and it is evident that any transition time between states represents a time in which the device appears as some unspecified nonlinear resistance. This is undesireable, since this behavior causes conversion loss, and subjects the mixer to IM generation while in a transitional state. In practice it is difficult to say much about the transition time behavior, and the greater part of the effort here will be expended on calculating departures from ideal models based on parasitic impedances, with perfect square wave switching assumed.

## PARASITIC IMPEDANCE ANALYSIS

The following analysis will be a first cut at describing the effects of the parasitic impedances. The mixer will first be analyzed under the assumption that the off state of the devices is percect (no reverse current) and that there is a small but measureable voltage drop across the on devices. The assumptions are then reversed, with the effects of off-state current flow analyzed with the voltage across the on devices equal to zero. These

approximate solutions should be good enough for estimates of the conversion loss and IM generation levels of the mixer (though a slightly different approach is more rewarding in the investigation of conversion loss). A simple extension of the analysis will allow an iterative solution of the exact values of these solutions.

It will be worthwhile to separate the common mode and difference mode voltages and currents as measured on the terminals of the mixer.(Fig.7, 9) In addition the parasitic impedances are separated into odd-order and even-order portions, with the parasitic voltages or currents also split into odd and even-order components.

For Fig. 7 the mixer will be analyzed in terms of total voltage drops around the input and output paths for both states of the mixer bridge; this allows us to separate the effects of the terms which are converted by the mixer and those which are not. The voltage drop across the on devices is written as a function of current; dividing them by their instantaneous currents defines them as extermal impedances.

For state 1, with devices $D_1$ and $D_2$ on and $D_3$ and $D_4$ off, $I_1=I_2$

$$V_{1c} + \frac{V_{1d}}{2} + v_1 - \frac{V_{2d}}{2} - V_{2c} = 0 \tag{28}$$

$$V_{1c} - \frac{V_{1d}}{2} + v_2 + \frac{V_{2d}}{2} - V_{2c} = 0 \tag{29}$$

For state 2, with $D_3$ and $D_4$ on and $D_1$ and $D_2$ off, $I_1 = -I_2$

$$V_{1c} + \frac{V_{1d}}{2} + v_3 + \frac{V_{2d}}{2} - V_{2c} = 0 \tag{30}$$

$$V_{1c} - \frac{V_{1d}}{2} + v_4 - \frac{V_{2d}}{2} - V_{2c} = 0 \tag{31}$$

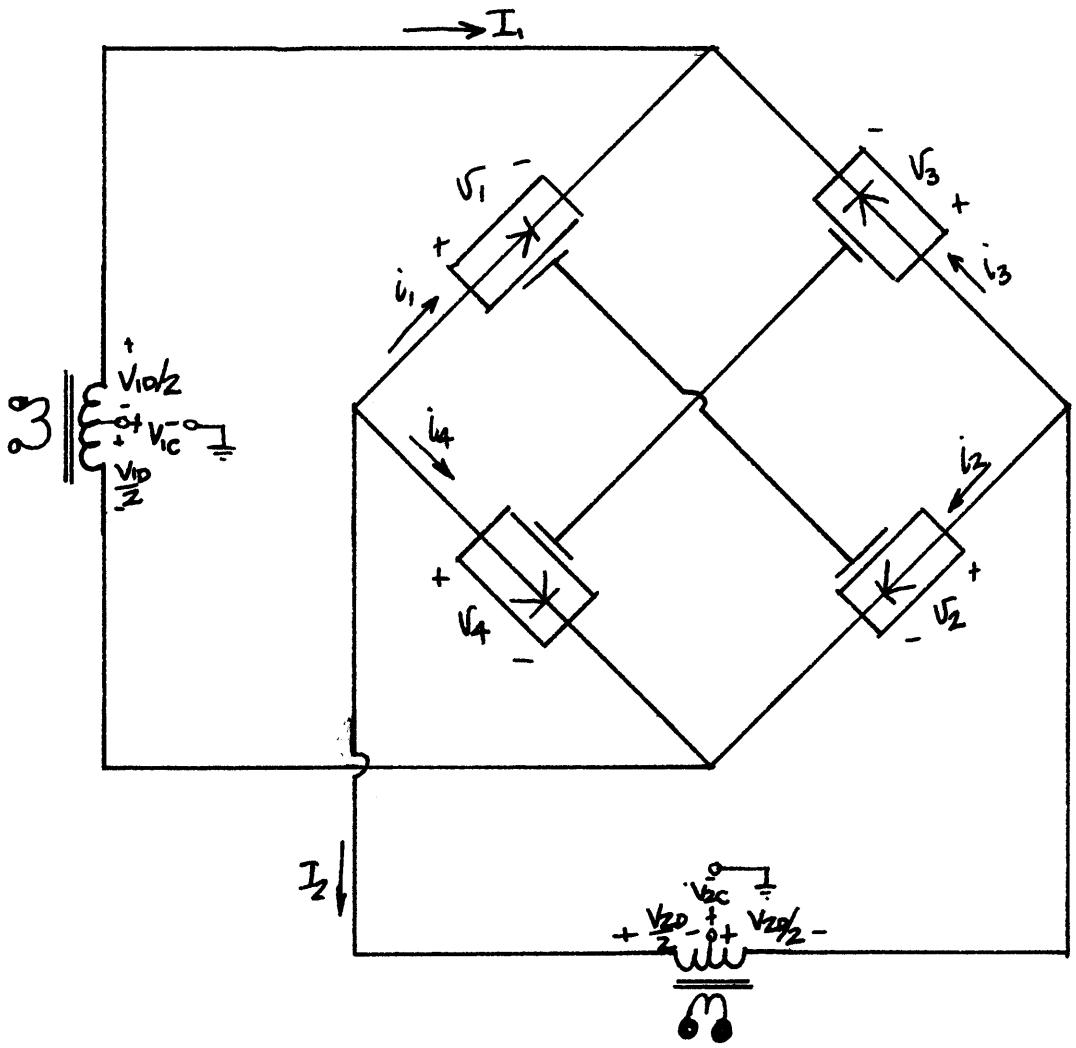


FIG. 7

The small v's represent the small voltage drop across the devices in the on state. It is assumed that they can be written as functions of their current; and by comparing the polarity of the currents that pass through the individual devices when they are on, we may write

$$v_1 = f(-I_1) = f(-I_2) \tag{32}$$

$$v_2 = f(I_1) = f(I_2) \tag{33}$$

$$v_3 = f(-I_1) = f(I_2) \tag{34}$$

$$v_4 = f(I_1) = f(-I_2) \tag{35}$$

Then $v_1 = (1/2)[\ f(-I_1) + f(-I_2)\ ]$ (36)

and similarly for the other $v_i$.

Let $f(I) = f_e(I) + f_o(I)$ where (37)

$$f_e(-I) = f_e(I) \quad \text{and} \quad f_o(-I) = -f_o(I) \tag{38}$$

The state 1 constraints become

$$V_{1c} + \frac{V_{1d}}{2} + \frac{1}{2}[\ f_e(-I_1)+f_o(-I_1) + f_e(-I_2) + f_o(-I_2)\ ] - \frac{V_{2d}}{2} - V_{2c} = 0 \tag{39}$$

$$V_{1c} - \frac{V_{1d}}{2} + \frac{1}{2}[f_e(I_1) + f_o(I_1) + f_e(I_2) + f_o(I_2)] + \frac{V_{2d}}{2} - V_{2c} = 0 \tag{40}$$

Adding (39) and (40) gives

$$V_{1c} + (1/2)f_e(I_1) = V_{2c} - (1/2)f_e(I_2) \tag{41}$$

while subtracting gives

$$V_{1d} - f_o(I_1) = V_{2d} + f_o(I_2) \tag{42}$$

Following the same procedure for state 2 gives

$$V_{1c} + (1/2)f_e(I_1) = V_{2c} - (1/2)f_e(I_2) \tag{43}$$

$$V_{1d} - f_o(I_1) = -[\ V_{2d} + f_o(I_2)\ ] \tag{44}$$

It becomes clear that the even order voltage components are not affected by the state change, while the odd-order components have reversed polarity.

Therefore the odd-order voltages must be in series with the input voltage, while the even-order voltages remain unconverted, and do not show up in the total input voltage. The effects of these on-state voltages can be removed from the mixer and modeled by external voltage sources, or (if divided by their currents $I_1$ and $I_2$) as impedances. (Fig. 8)

A similar method is used for finding the effects of the off-state current flow, based on the common-mode and difference-mode currents indicated in Fig. 9. Some addition has already taken place at the input and output transformers, with the result that the form of the equations will be a bit different with the given variables; however, the equations are consistent with the devices and circuits, and the results are similar: The even-order currents are not converted, and show up in the center of the input and output transformers, while the odd-order terms add or subtract to the input currents, and their effects are converted. In detail, the method involves summing the currents at each node; for state 1, nodes p and q collapse to node pq and nodes r and s to node rs (Fig. 10a); and for state 2, collapse to nodes qr and ps (Fig. 10b). The effects of the even-order and odd-order terms $h_e(V)$ and $h_o(V)$ are shown in Fig. 11.

The result is a first-order approximation to the effects of the parasitic impedances. For a more accurate iterative solution, the voltage across the h functions must be modified by the voltage drops of the on devices. The external-source derivations were done independently, and the total characterization follows Fig. 12. The h function across the input and output now becomes $h_o[V - 2(\frac{f_o(I)}{2})]$ and the f becomes $f_o[I - h_o(V)]$. The substitutions are continued until the values converge.

FIG. 8

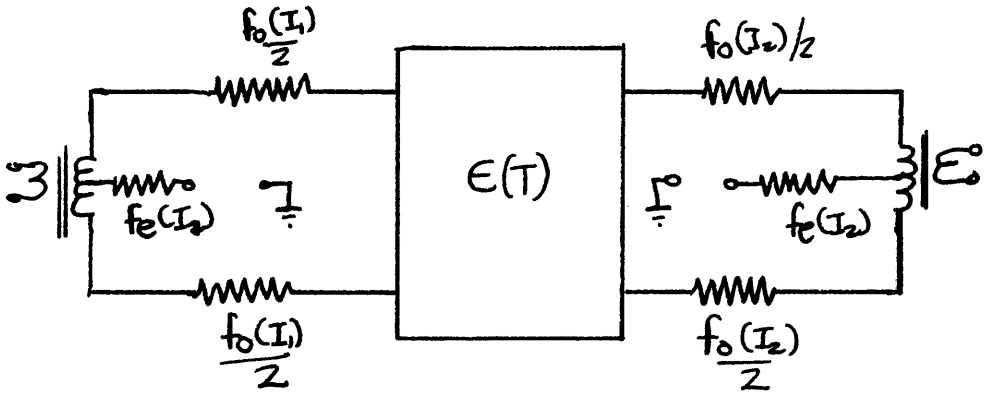


ON-STATE VOLTAGE DROPS

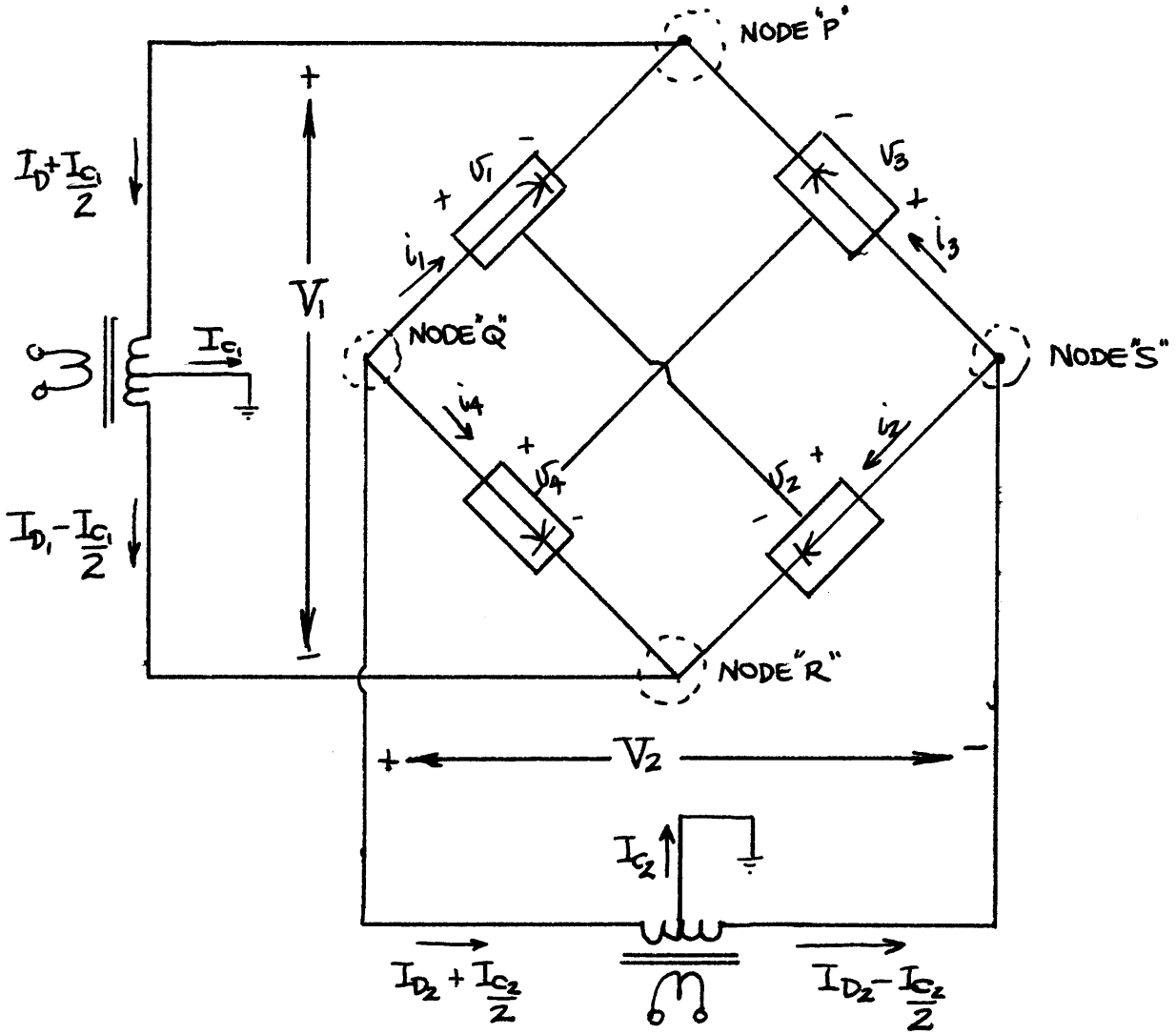
NODE "P"
NODE "Q"
NODE "S"
NODE "R"
$I_D + \frac{I_{C_1}}{2}$
$I_{D_1} - \frac{I_{C_1}}{2}$
$I_{C_1}$
$V_1$
$v_1$
$v_2$
$v_3$
$v_4$
$i_1$
$i_2$
$i_3$
$i_4$
$V_2$
$I_{C_2}$
$I_{D_2} + \frac{I_{C_2}}{2}$
$I_{D_2} - \frac{I_{C_2}}{2}$

FIG. 9

FIG. 10a

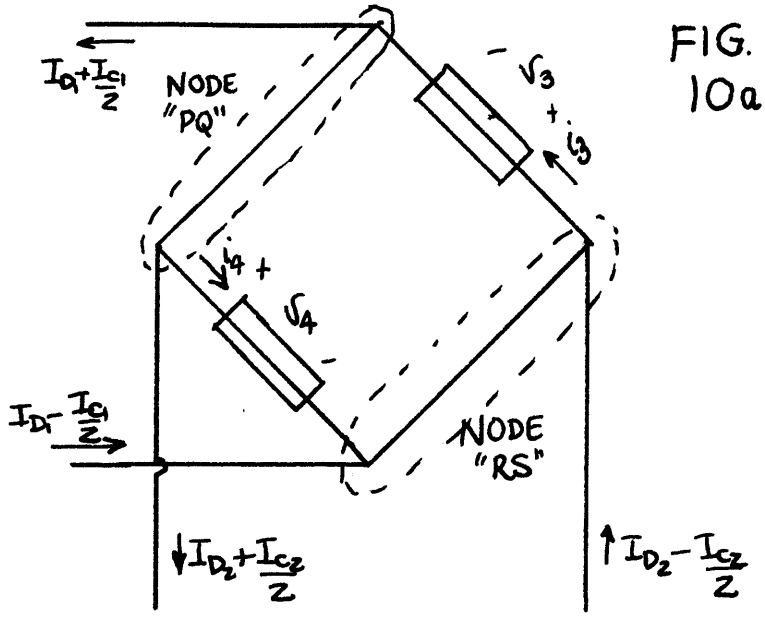


STATE 1

FIG. 10b

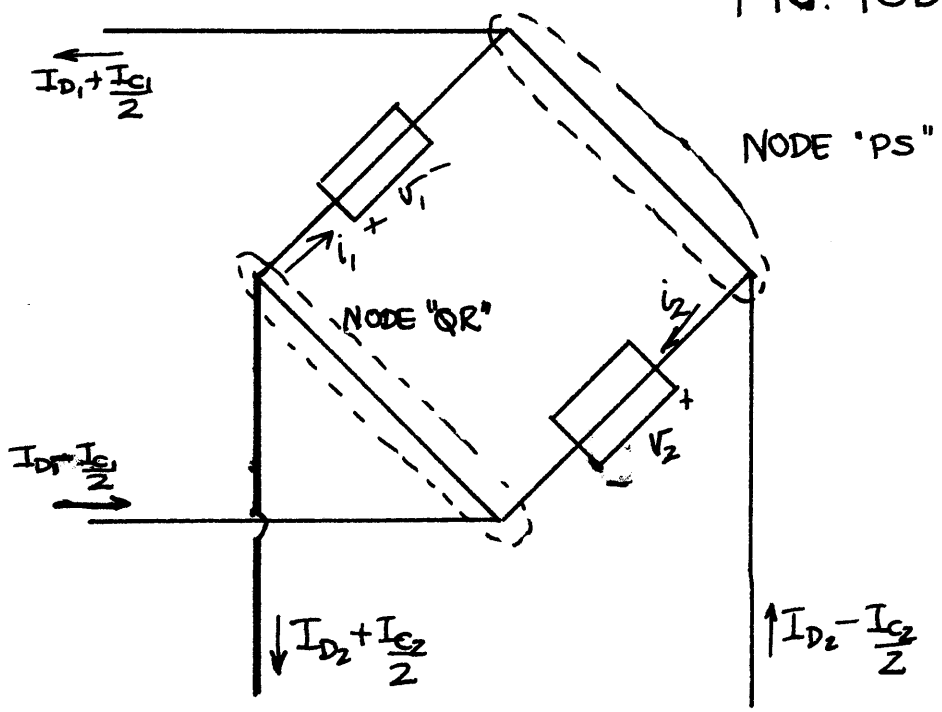


STATE 2

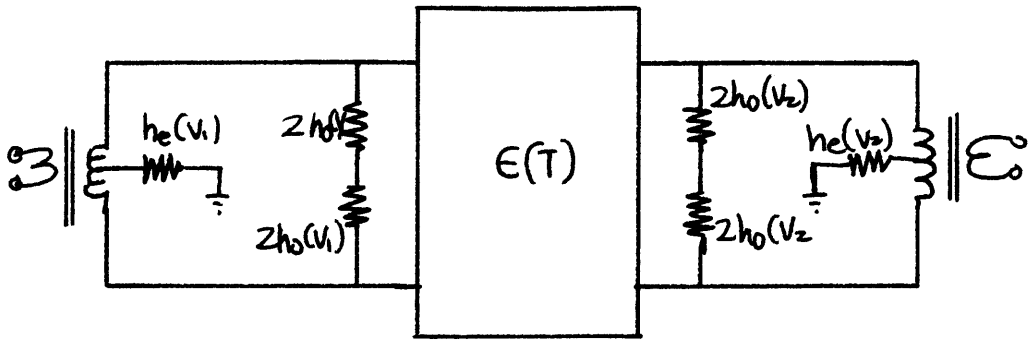
$h_e(V_1)$
$2h_o(V_1)$
$2h_o(V_1)$
$\epsilon(T)$
$2h_o(V_2)$
$h_e(V_2)$
$2h_o(V_2)$

FIG. 11

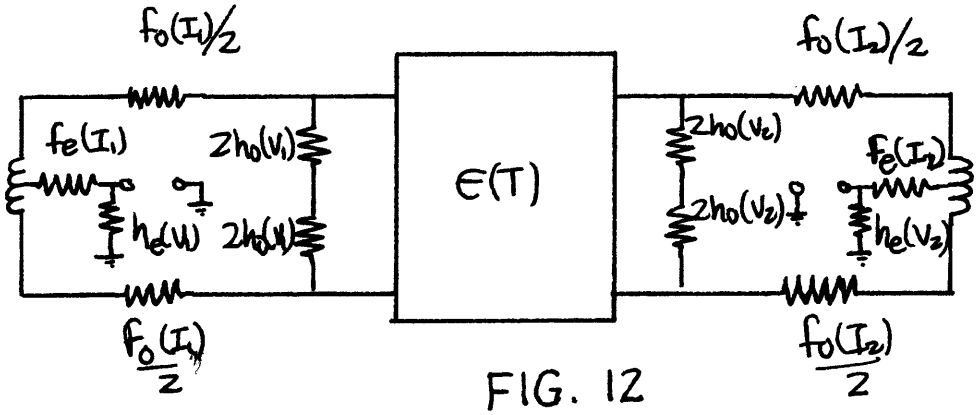
$f_o(I_1)/2$
$f_e(I_1)$
$2h_o(V_1)$
$h_e(V_1)$
$2h_o(V_1)$
$f_o(I_1)/2$
$\epsilon(T)$
$f_o(I_2)/2$
$2h_o(V_2)$
$f_e(I_2)$
$2h_o(V_2)$
$h_e(V_2)$
$f_o(I_2)/2$

FIG. 12

The intermodulation products generated in the parasitic impedances have one important difference from the IM as analyzed in the simple nonlinear resistance. Since the frequency conversion follows the odd-order impedance at the input, one pass through the $\epsilon(T)$ conversion is sufficient for IM generation at the output. Similarly, the third-order term in the parasitic impedance at the output takes the undesired signals, converted to frequencies $\omega_{LO} \pm \omega_i$ and $\omega_{LO} \pm \omega_j$, and converts them to frequencies of the form $2[\omega_{LO} \pm \omega_i] \pm [\omega_{LO} \pm \omega_j]$, which includes a component at $\omega_{LO} - [2\omega_i \pm \omega_j] = \omega_{IF}$. Both odd-order impedances, on input and output, contribute to the generation of third-order IM.

## CONVERSION LOSS

It is clear that the conversion loss of the mixer with parasitic impedances will be greater than zero db, since the real parts of the on and off device impedances represent dissipated power. In practice the major contribution to conversion loss is the on-state resistance, in the FET fixed by the minimum channel resistance. The off-state series resistance is on the order of several thousand ohms or more, and the capacitive reactance to ground is of the same magnitude, in a typical FET. A good estimate of the conversion loss, therefore, simply models the mixer as the input voltage source (with its internal generator resistance $R_g$) in series with the on-state resistance $R_{ON}$ (or $Z_{ON}$ for general solution). The conversion loss is a difficult quantity to measure, depending on an exact knowledge of the mixer output impedance; more readily available is the Transducer loss, the ratio of available input power to actual output power into the load resistance $R_L$. The available input power is $\frac{|V_{IN}|^2}{4R_g}$ while the actual output power is $\frac{|V_{OUT}|^2}{2R_L}$. If we

assume the frequency terminations used in the experimental work, of short circuited sum at the output and open circuited image at the input, the output impedance $Z_{OUT} = \frac{\pi^2}{4}[R_g + Z_{ON}]$ (Fig. 13a and 13b) The input voltage $V_{IN}$ transforms to a voltage generator of $\frac{2}{\pi}V_{IN}$ in series with $Z_{OUT}$, and the output voltage

$$V_{OUT} = \frac{(2/\pi)V_{IN}R_L}{R_L + Z_{ON} + \frac{4}{\pi^2}[Z_{ON}+R_g]} \tag{45}$$

$$L_T = \frac{P_{IN}}{P_{OUT}} = \frac{\pi^2[R_L + Z_{ON} + (4/\pi^2)(R_g + Z_{ON})]^2}{8R_LR_g} \tag{46}$$

## SIGNAL LEVEL PERTURBATIONS

There is another limitation on the power levels which the mixer can handle before the IM generated becomes measureable. The mixer has been characterized as if the only variables controlling the operating point were the switching waveform amplitudes. However, with high signal levels--both desired and undesired signals--The operating point will vary with the instantaneous amplitudes of the input signals. The problems arise when the switched states do not have an infinite range of voltage or current available over which the state remains unchanged, and the signal level on the devices can drive them into non-linear regions. (Fig. 14) This mode of IM generation most closely approximates the normal modes of IM generation in conventional mixers, and it is not surprising that the best results and lowest IM occur with devices designed for minimum IM in conventional mixers. This large linear range in normal circuitry is another of the reasons for the choice of FETs for the switched devices.[9,10,11,12,13,14,15] The normal on

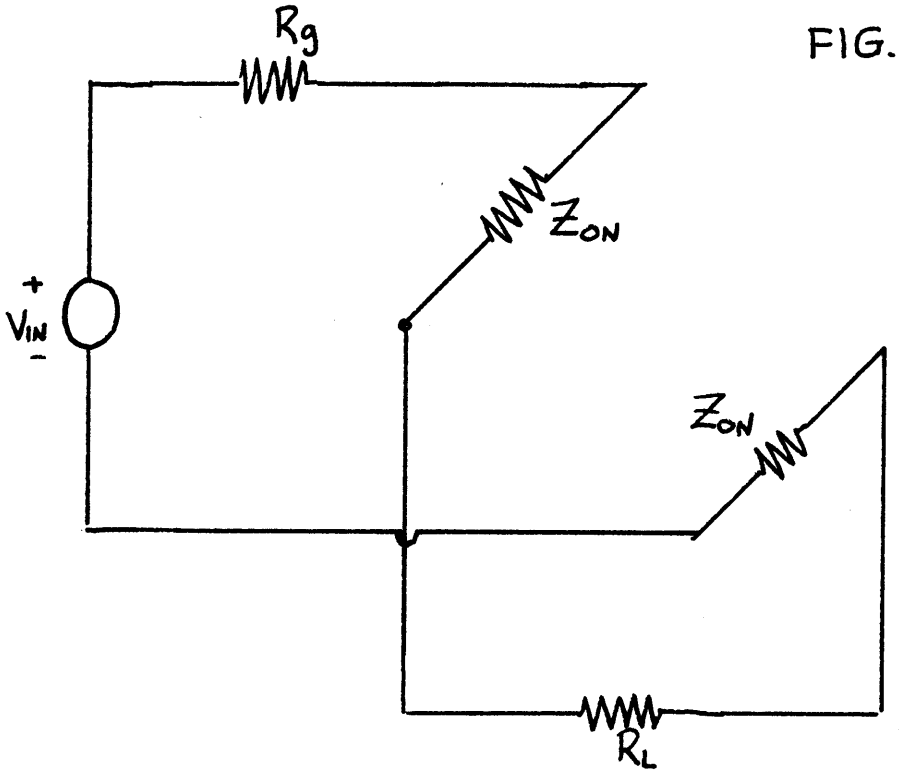


FIG. 13a

STATE ① WITH $Z_{ON} > 0$ $Z_{OFF} = \infty$

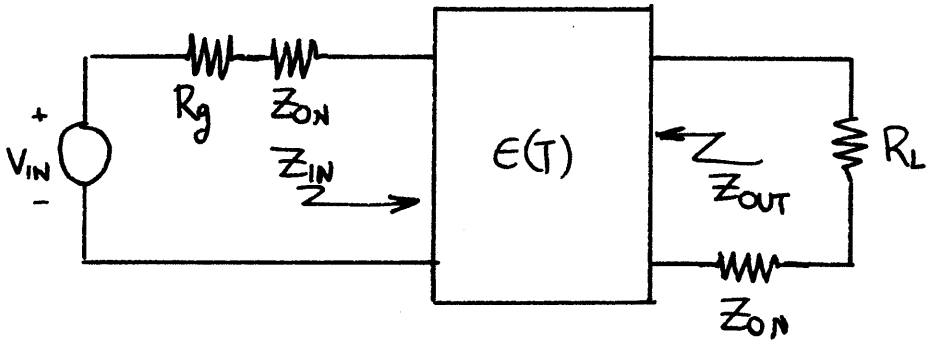


FIG. 13b

state of an FET has a resistance greater than zero, on the resistive portion of the $I_{Drain}$ vs. $V_{DS}$ curve. For large signals on the source (as in the bridge mixer) the operating point moves along the characteristic (fixed $V_g$) into the nonlinear region, generating IM.

## TRANSITION TIME BEHAVIOR

The final limitation on dynamic range comes from the transition times associated with any real-world switching system. While the optimum LO waveform is a perfect square wave, the combination of high required LO power and relatively high frequency (on the order of $10^7$ Hz) make such a wave difficult to obtain. Much more likely to occur is a clipped sine wave (Fig. 15) with fairly long transition times, on the order of T/6 each way. This means that the FETs spend a good fraction of time traveling through a succession of operating points somewhere in the normal operating region of their characteristic curves, over a general area (Fig. 16) fixed by the amplitude of the input signals at the source and the approximate path of the operating point between the on and off states. The Amplitude of the intermodulation will be greatest when the FET is somewhere near the middle of the transition, and the output amplitude may be approximated by "triangles" of base width $t_{trans}$ and period T/2.

## SUMMARY OF THEORETICAL ANALYSIS

The dynamic range of the balanced-bridge mixer is thus seen to be the range over which the mixer can operate without running into the device limitations. Conversion loss and system noise figure set the lower limit on the

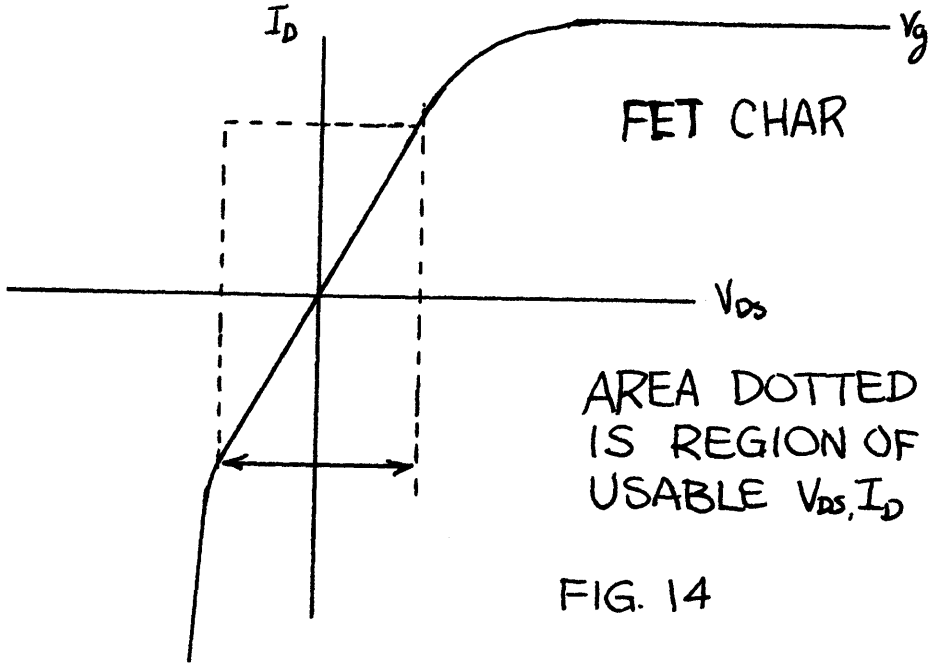
$I_D$
$V_g$
FET CHAR
$V_{DS}$
AREA DOTTED IS REGION OF USABLE $V_{DS}, I_D$

FIG. 14

FIG. 15

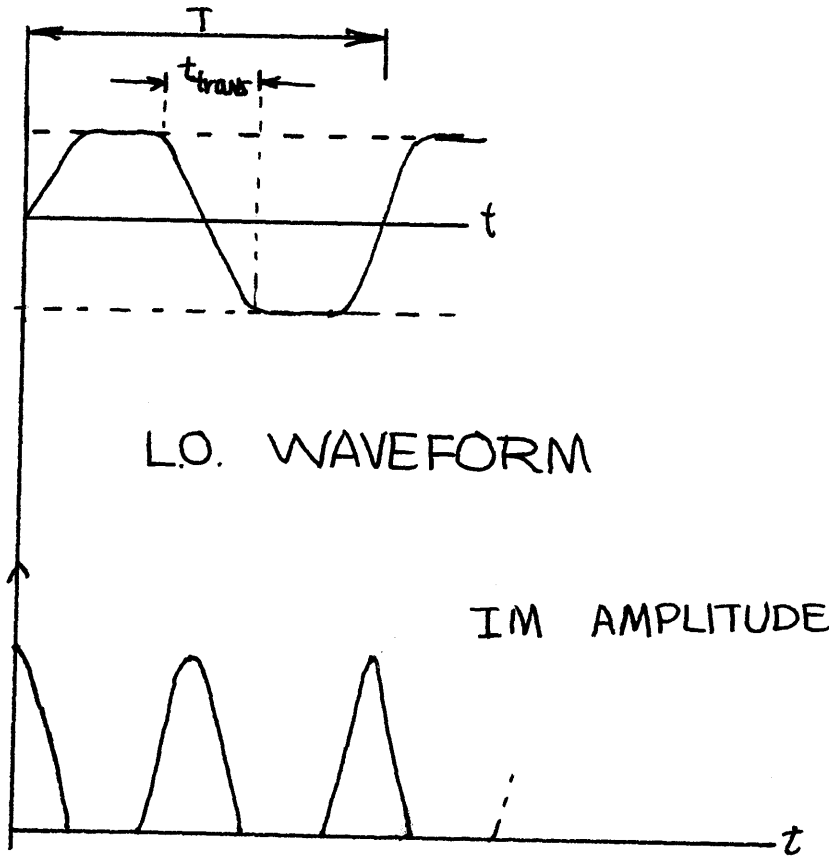
T
$t_{trans}$
t
L.O. WAVEFORM
IM AMPLITUDE
t

FIG. 16

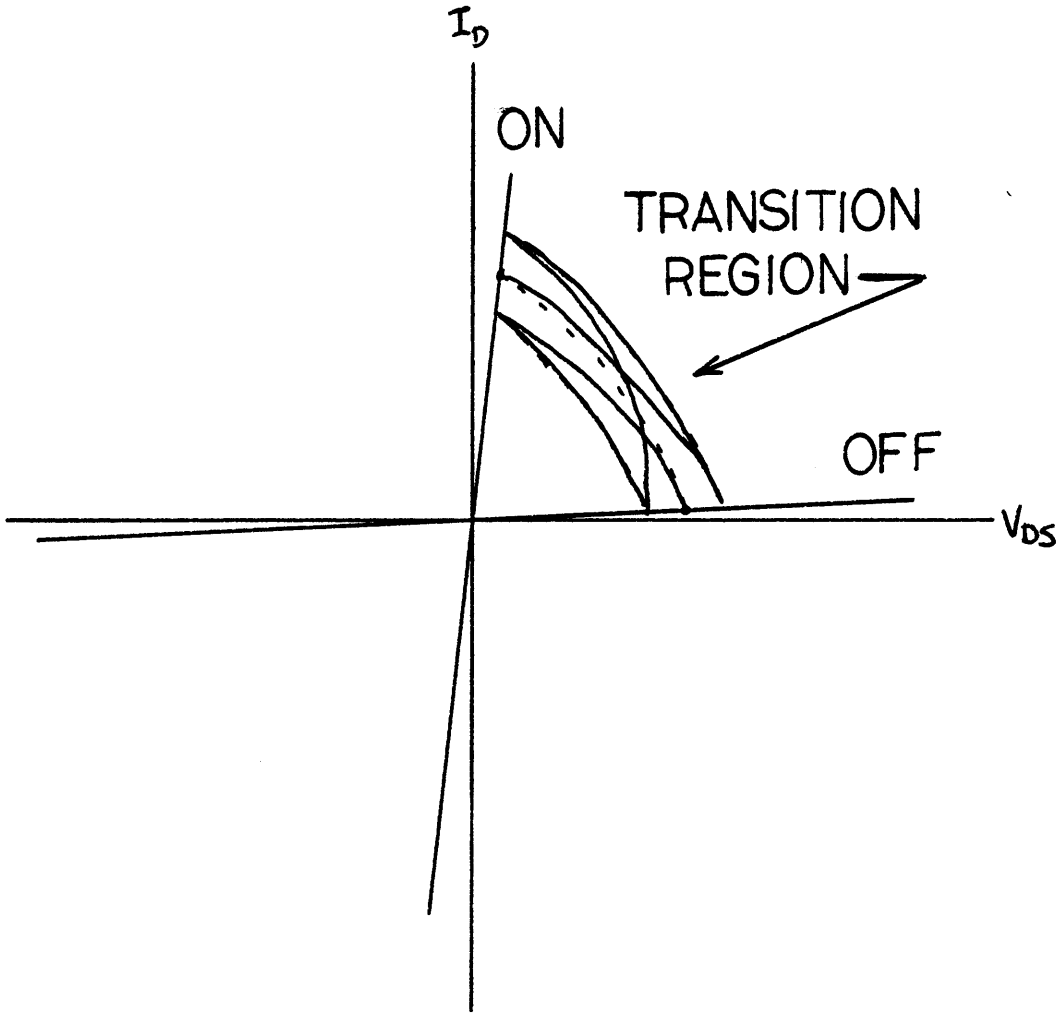

sensitivity, and intermodulation generated by parasitic impedances, signal-level-produced nonlinearities, and transition-time effects sets the upper limit of the dynamic range.

This portion of the thesis has developed the mathematical theory behind an unusual mixer circuit, and shown that the ideal model is free from IM and implies zero conversion loss. The departures from the ideal case have been analyzed in more or less detail, and methods have been developed for estimating the dynamic range of the resulting mixer from experimental measurements of the fundamental device limits.

The following section of this thesis is devoted to a description and explanation of the experiments conducted to measure the performance of a real-world version of this mixer, operating in a single-sideband receiver.

# EXPERIMENTAL

## ORGANIZATION AND EQUIPMENT

Experimental systems should be capable of accurate measurement of as many of the experimental variables as possible. While the major concern of this thesis is that the receiver have the greatest possible dynamic range with the best possible sensitivity,we must also specify and measure the performance in terms of bandwidth, information and modulation modes, detection capabilities, and output mechanisms.

The basic receiver consisted of the mixer, fed directly by the signal generators through a variable attenuator and a low pass filter. The local oscillator power was taken from a Boonton power amplifier operating at 40MHz, with a Kay Model $\pi$ Sweep Frequency Generator feeding the amplifier. The IF output was fed into a rebuilt commercial crystal filter, modified for wider dynamic range and greater resistance to IM. This was followed by a "black box" IF amplifier and another crystal filter, unmodified. The detection devices varied; for measurement of dynamic range, a Collins R-390 receiver was used as a detector with built-in frequency meter and relative power meter. A phase detector, with its own 30 MHz local oscillator, was also built, based on the mixer design, and used with a variety of audio amplifiers.

Receiver sensitivity was measured as the minimum discernible signal, for a 10 db S+N/N ratio in the R-390, at 1 KHz bandwidth. (Fig. 17) With no signal input to the mixer, the R-390 BFO was turned on and RF gain (on manual gain control) was set to give a noise level in the Line Level meter of 10 db below the arbitrary 0 db level. The GR 805C oscillator was set for $V_{out}$= 2.8 volts rms which corresponds, at 50 ohm impedance level, to +22 dbm. (All sensitivity measurements were conducted at $f_s$ = 10.0 MHz.)

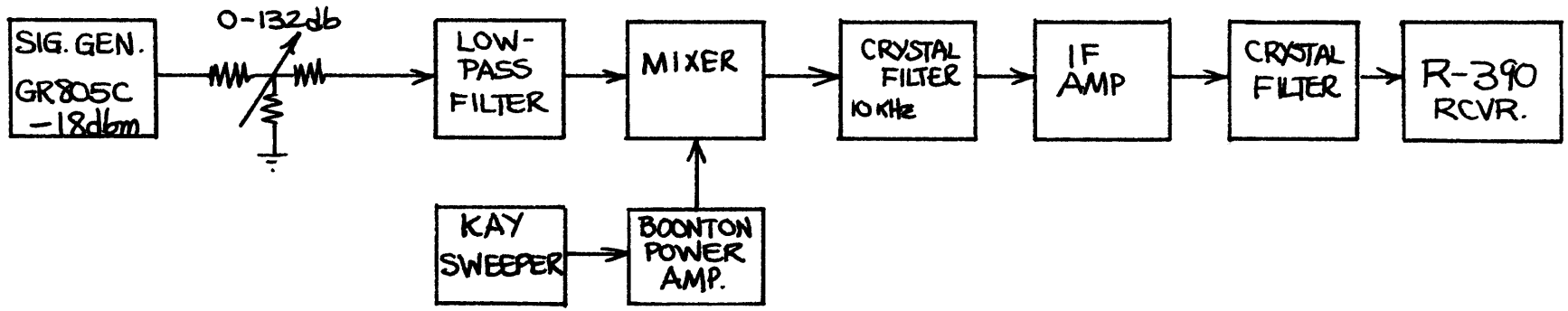


SENSITIVITY MEASUREMENT

FIG. 17

The variable attenuator was set for a measured signal+noise to noise ratio in the R-390 of 10db; the signal sensitivity is then $db_{atten}$-22dbm = sens.(dbm)

Most of the intermodulation measurements were made with third-order products, since for normal power levels these will be dominant over higher-order products. The first signal generator was retuned to a siutable $\omega_i$ and a second GR 805C oscillator, tuned to a suitable $\omega_j$ such that $2\omega_i-\omega_j=10.0$ MHz, was fed into the mixer. The second generator was adjusted for equal signal level, and both generators were attenuated equal amounts at all times. The R-390 was again set for -10db relative on Line Level meter, and the attenuation on the GR oscillators set for a third-order IM signal level 10 db above the noise level, or 0 db relative. This gave a measure of the required signal power (in dbm) of the undesired signals for IM to be produced with a 10 db [S+N]/N ratio. The dynamic range is then the difference between the IM power level (dbm) and the signal sensitivity (in dbm) plus 3 db (because the total power of the IM two-tone is twice as great (+3db) as the signal power level). The dynamic range is clearly a measure of how large nearby undesired signals can be while the desired signal is the minimum possible, the 10 db [S+N]/N signal. (Fig. 18)

For example, suppose the 10.0 MHz sensitivity is 105 db below the +22 dbm input signal, for 10 db signal plus noise to noise ratio. Then Sens.= -83dbm. If the required IM level is 33 db below the 2.8 volt signal voltage = -11 dbm, the dynamic range is +83 dbm +[-11dbm] + 3db = 75 db.

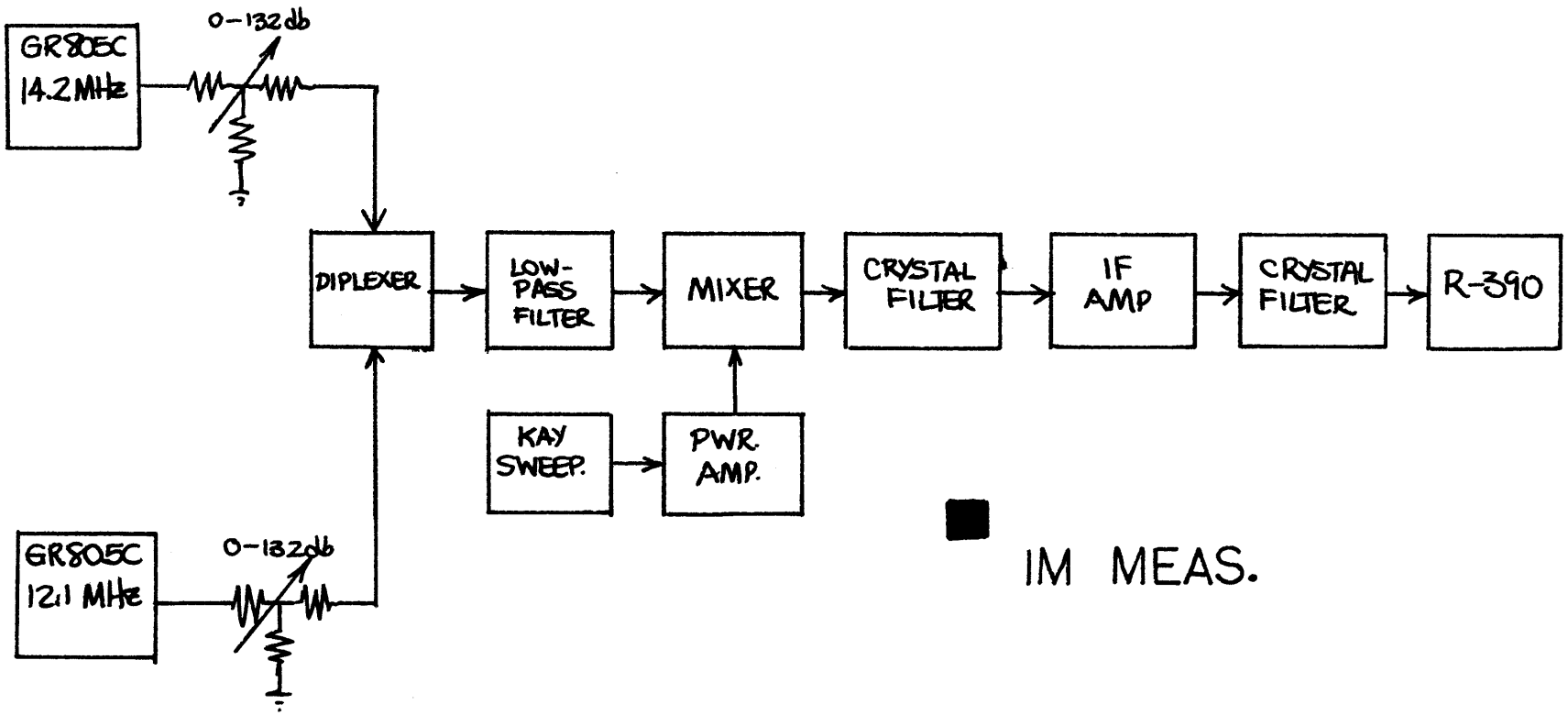


IM MEAS.

FIG. 18

## DISCUSSION OF SUBUNITS

### MIXER

The mixer used in the experimental version of this receiver was based on a bridge of four FETs. The transistors used were Fairchild 2N4067 MOS FETs, which come packaged in pairs in a single TO-5 can. The two FETs in each can have a common source, but separate gates and drains. The sixth lead into the case is the substrate. (An earlier version of this same mixer has been described by Lange.[16]) The RF input was applied to the common sources, and the IF output taken from the individual drains. The substrates were biased at +22.5 volts; although they are shown on Fig. 19 as separate leads for clarity, each pair has only one substrate lead. The paired leads are isolated by 100 Kilohm resistors. (This isolation is important, based on the FET physical model, of which more will be said later.) The local oscillator was fed into the gates of the four FETs in alternate pairs; the gates themselves are DC decoupled so that they may be DC biased individually by the gate bias network (Fig. 21). The LO input port is set at 50 ohms unbalanced input impedance by the 4:1 hybrid transmission line transformer and the two 100 ohm, two-watt resistors (Fig. 20) The output (IF) is short circuited at the sum frequency by a parallel-tuned LC circuit set for the 30 MHz IF frequency. (The input is open-circuited for the image frequency by the external low-pass filter). Both RF input and IF output ports are 50 ohm unbalanced, brought up to 200 ohm balanced inside the mixer by the 4:1 hybrids. (Fig. 19)

### CRYSTAL FILTERS

The crystal filters used in this receiver are based on two commercial five-pole filters made by the CTS Knights Co. The specifications are 6 db

FIG. 19

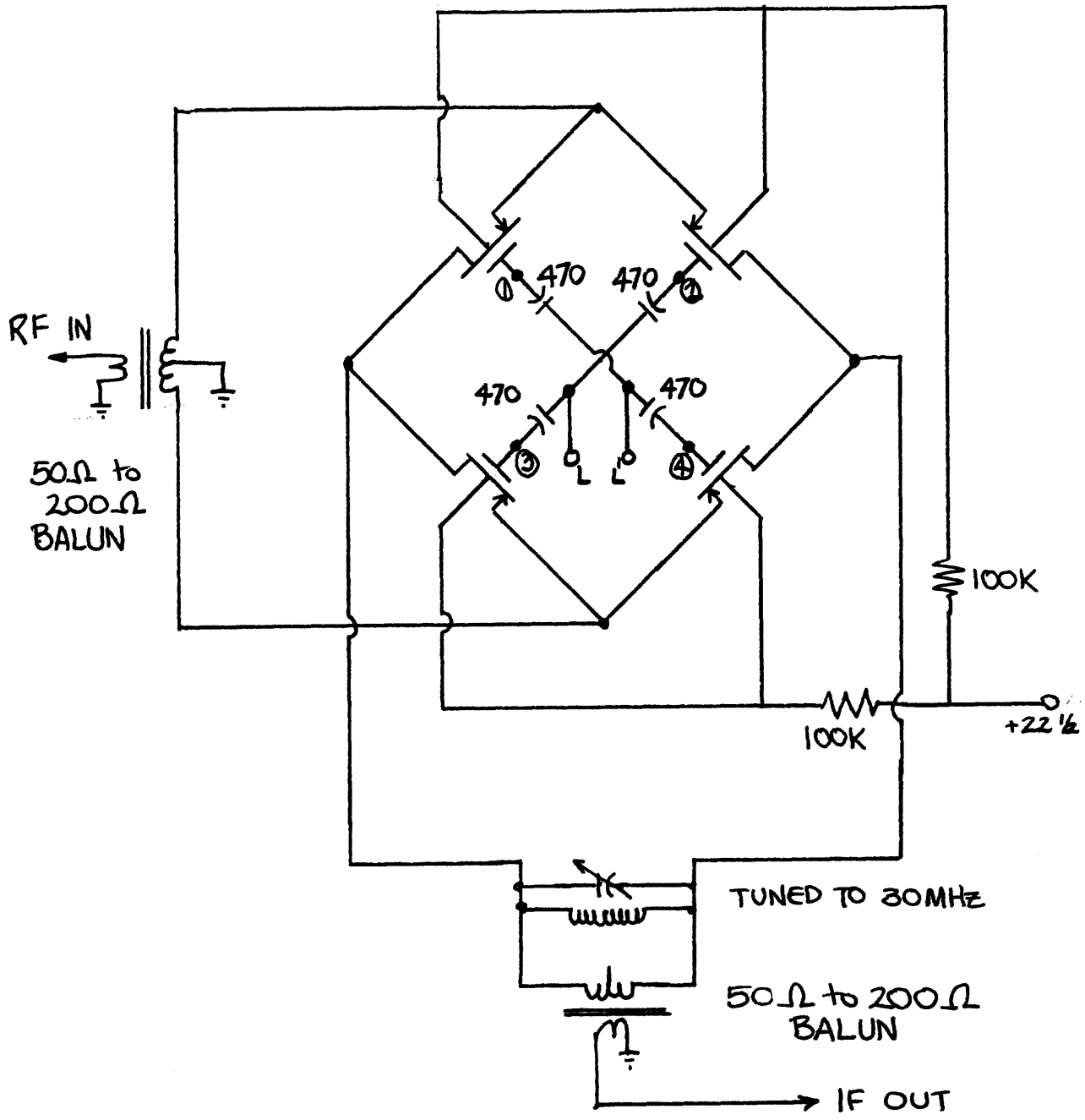
RF IN
50Ω to
200Ω
BALUN
470
470
470
470
100K
100K
+22½
TUNED TO 30MHz
50Ω to 200Ω
BALUN
IF OUT

MIXER

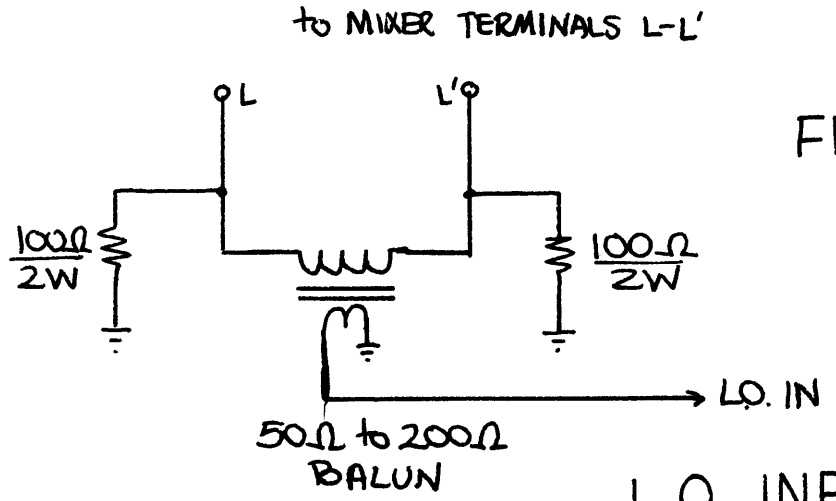


FIG. 20

L.O. INPUT NETWORK

FIG. 21

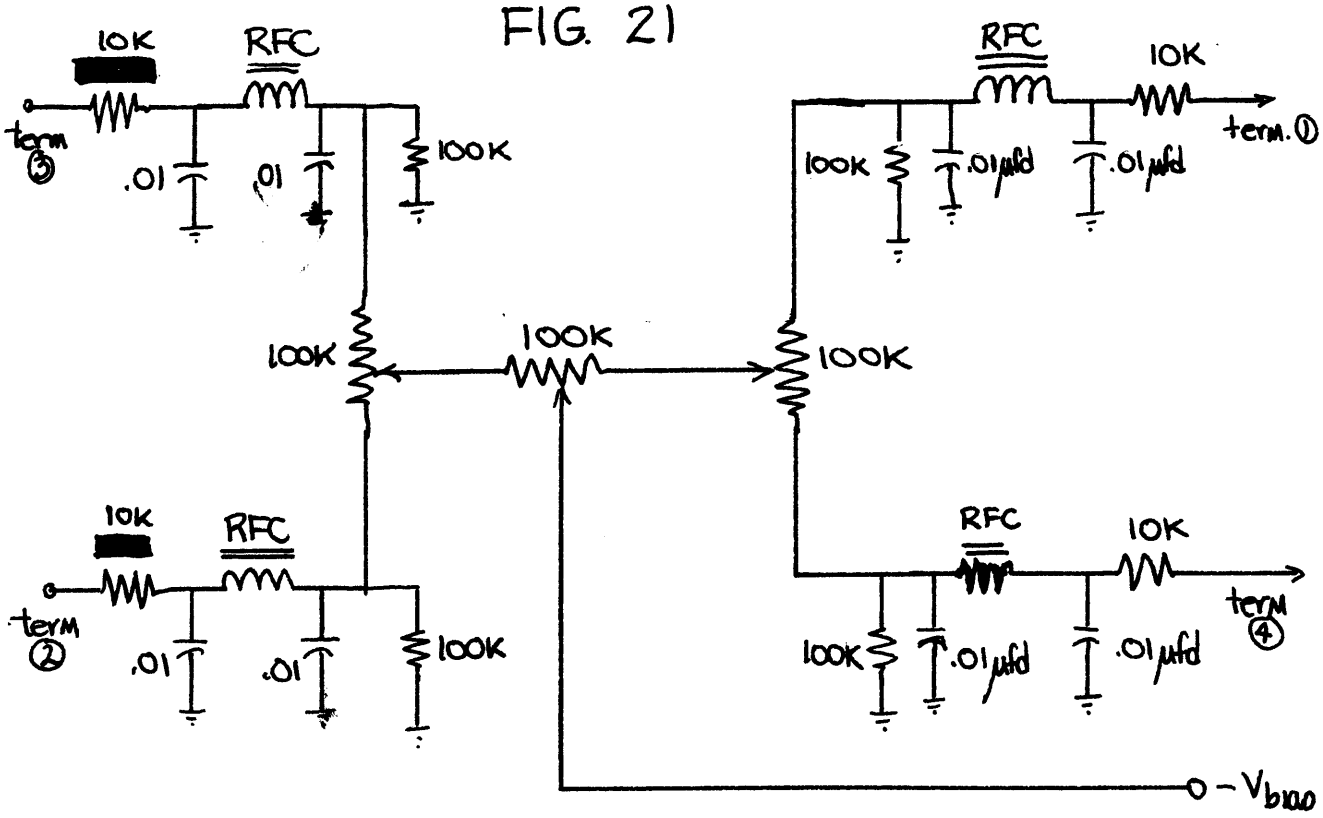


GATE BIAS NETWORK

passband of 10 KHz at a center frequency of 30 MHz. The filter following the IF amplifier was used unmodified; the filter following the mixer was rebuilt in shielded enclosure to reduce out-of-band transmission, and new input and output impedance-matching networks added. The center-tapped coils were wound on larger powdered-iron (type SF) cores for lower internal IM, and the resonating capacitors replaced by Johannson 10-14 pfd. piston trimmer capacitors. The rebuilt filter is shown in Fig. 22; the commercial filter is the same, with two exceptions; the input variable capacitance in the ground return (and the output also) has been eliminated, and the variable capacitors are all fixed, with the exception of three trimmer capacitors resonating the three tapped powdered-iron coils to 30 MHz.

The rebuilt filter was aligned using the arrangement of Fig. 23; the passband was displayed in storage mode on the Tektronix 549 and the trimmer capacitors set for the desired passband.

Each filter had an in-band insertion loss of 5 db, and an out-of-band attenuation of approximately 65 db for the commercial filter, and greater than 80 db (the limit of the log amplifier) for the rebuilt filter. The cascade of both filters had a 6 db passband of 10.0 KHz, and a 60 db passband of approximately 20 KHz, giving a 6 to 60 db shape factor of two to one. The commercial filter followed the IF amplifier, so the effective insertion loss of the total selectivity circuitry was the 5 db insertion loss of the rebuilt filter (since the IF amplifier NF and power gain set the overall noise performance.)

## IF AMPLIFIER

The IF amplifier existed previous to the implementation of this thesis, and was used as a black box. Its power gain was approx. 30 db, and NF = 1.0 db.

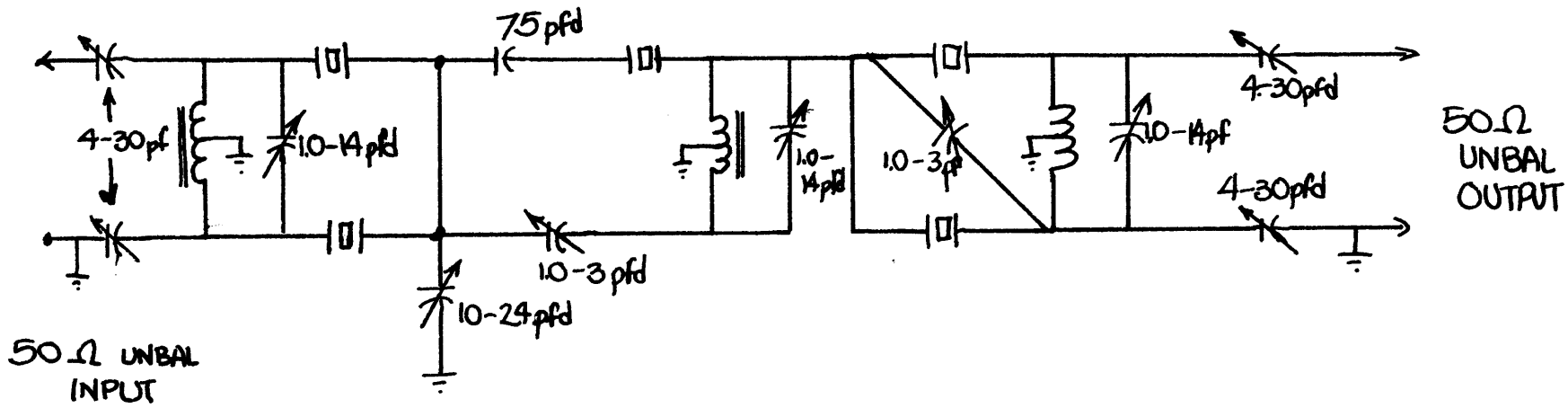


FIG. 22

REBUILT CRYSTAL FILTER

FIG. 23

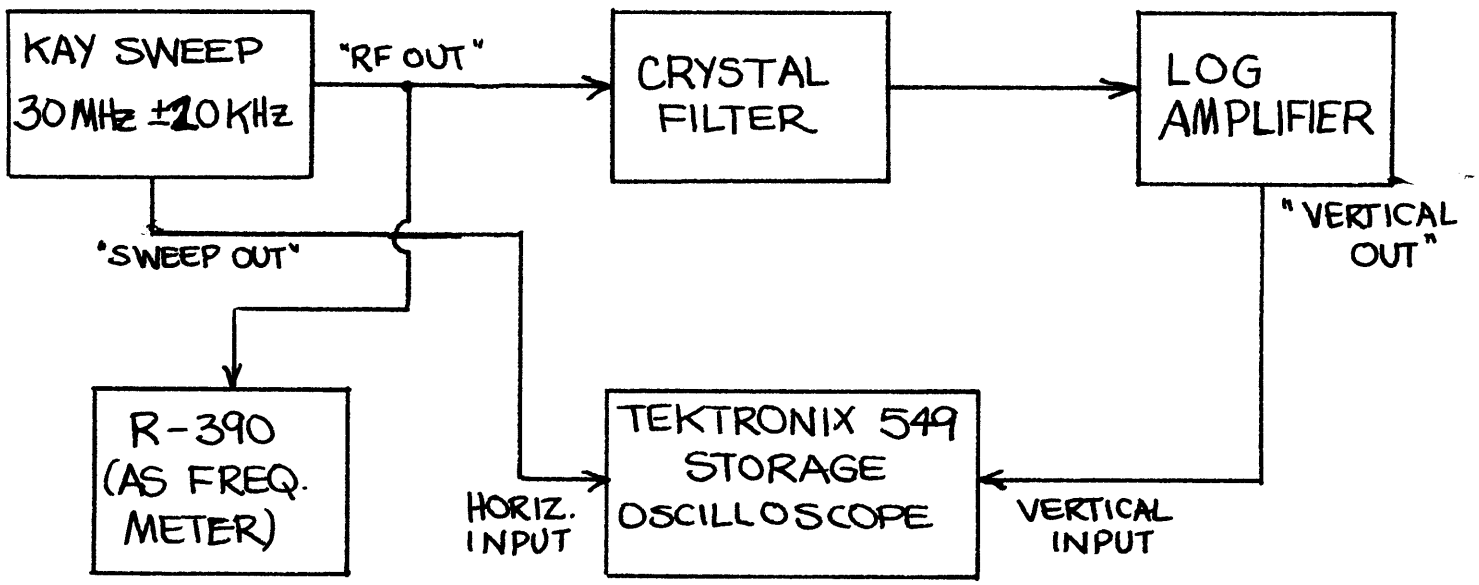


CRYSTAL FILTER PASSBAND MEASUREMENT AND ALIGNMENT

## LOW-PASS FILTER

The low-pass filter was designed to provide a transmission zero at the IF frequency of 30 MHz, and to show as an open circuit for the image frequency (between 30.5 and 60.0 MHz). The graph of attenuation versus frequency (Fig. 24) for the filter (Fig. 26) shows a peak attenuation at the $f_{\infty}$ = 30.0 MHz of greater than 90 db. The high-frequency behavior is approximated by a series inductor, providing the needed open circuit at the image frequency. The attenuation below the 30 MHz cutoff frequency is less than 0.5 db.

## DIPLEXER

The diplexer (Fig. 25) was designed to provide isolation between the two signal generators used in intermodulation measurements. The parallel tuned circuits present a high impedance to the signal from the opposite generator; without this isolation, the signals from opposing generators were feeding back through the reverse transconductance of the output tubes of the generators, and the internally generated intermodulation was masking the IM generated in the mixer. The attenuation of each LC circuit is approximately 30 db at the frequency of the opposite generator, and essentially zero at the generator output frequency.

## PHASE DETECTOR

With minor modifications the mixer will work as a phase (or product) detector for single-sideband signals. (Fig. 27a and 27b) The LO input network, operating at a single frequency of 30.0 MHz, raises the impedance level to 10,000 ohms balanced to allow lower LO power with the necessary 10 Volts RMS on the FET gates. The output network short-circuits the sum

FIG. 24

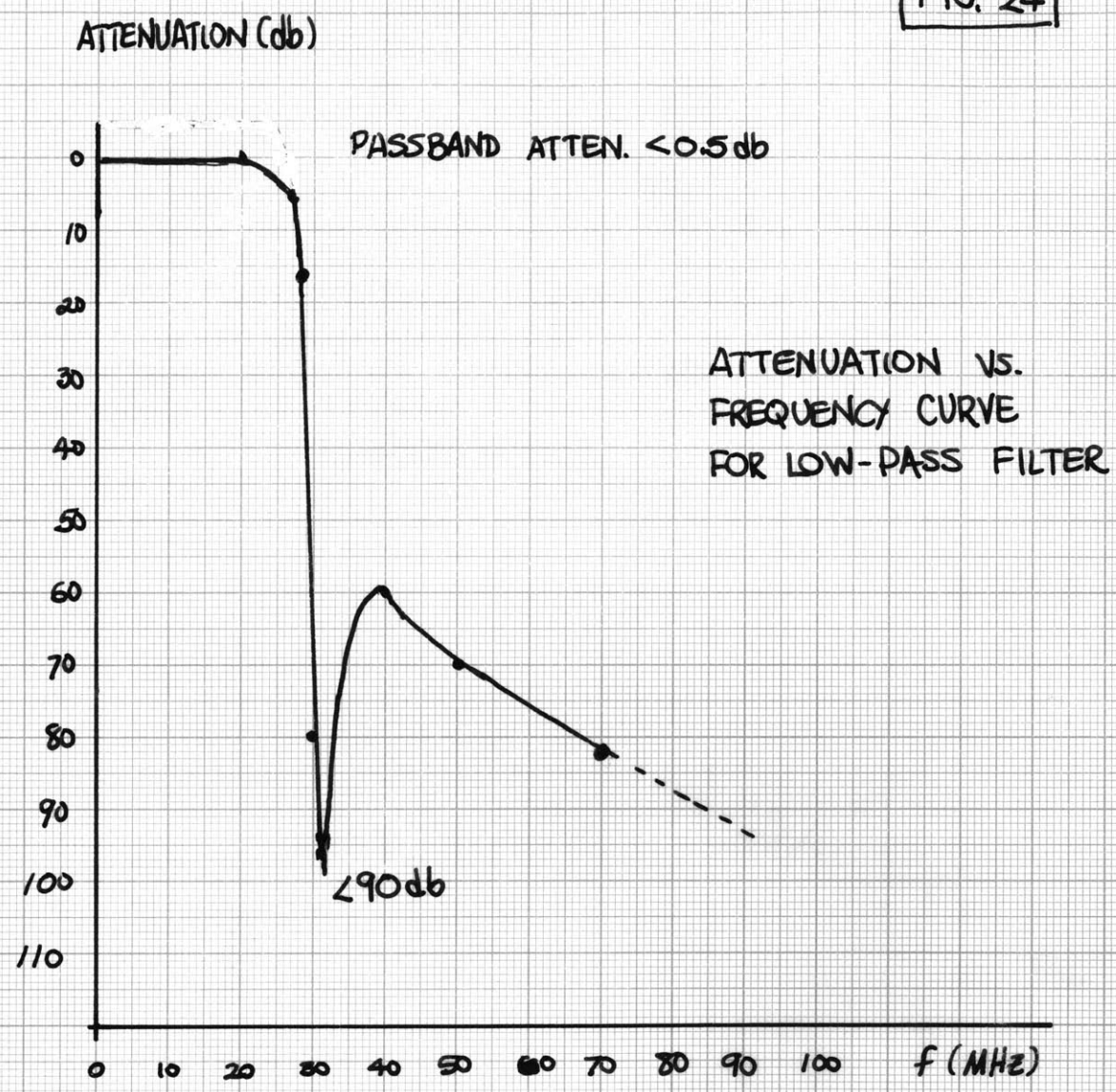


data taken by R.R. Rafise 20 JUNE 1967

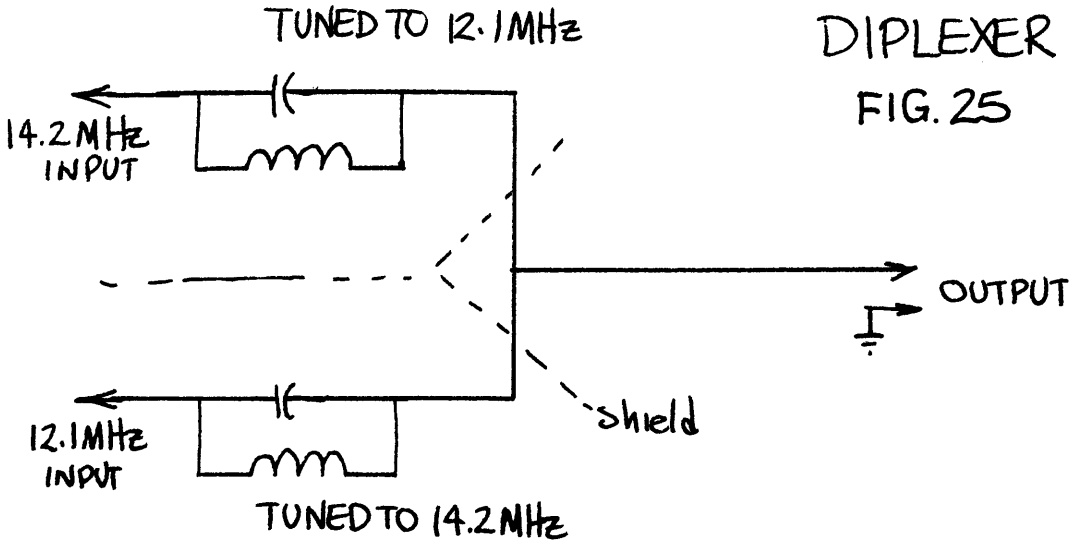


DIPLEXER

FIG. 25

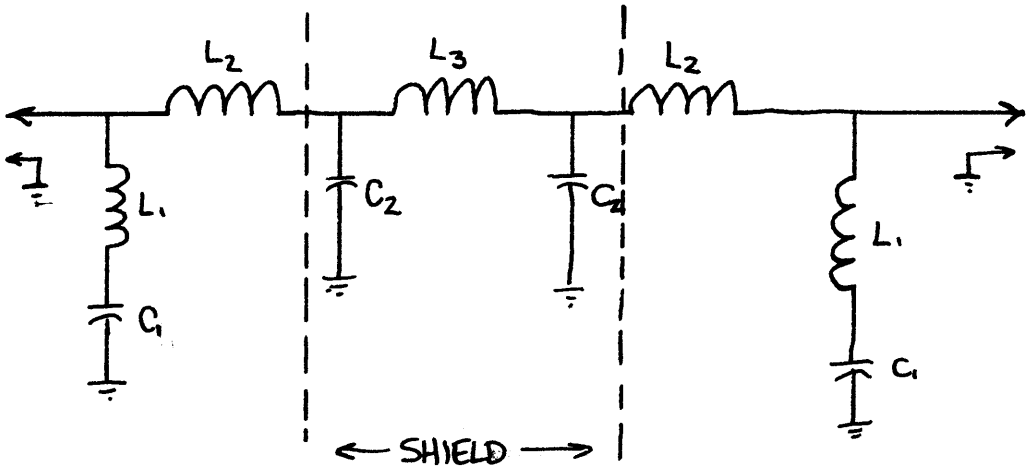


LOW PASS FILTER

$Z_0 = 50\Omega$ $f_{co} = 30.0$ MHz

FIG. 26

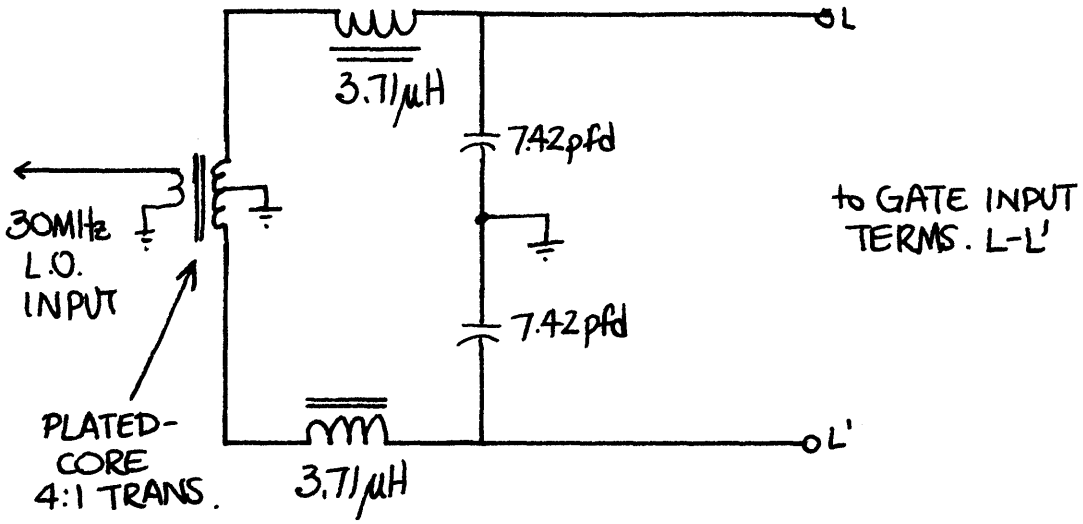


FIG 27a PHASE DETECTOR L.O. INPUT NETWORK

FIG. 27b OUTPUT NETWORK

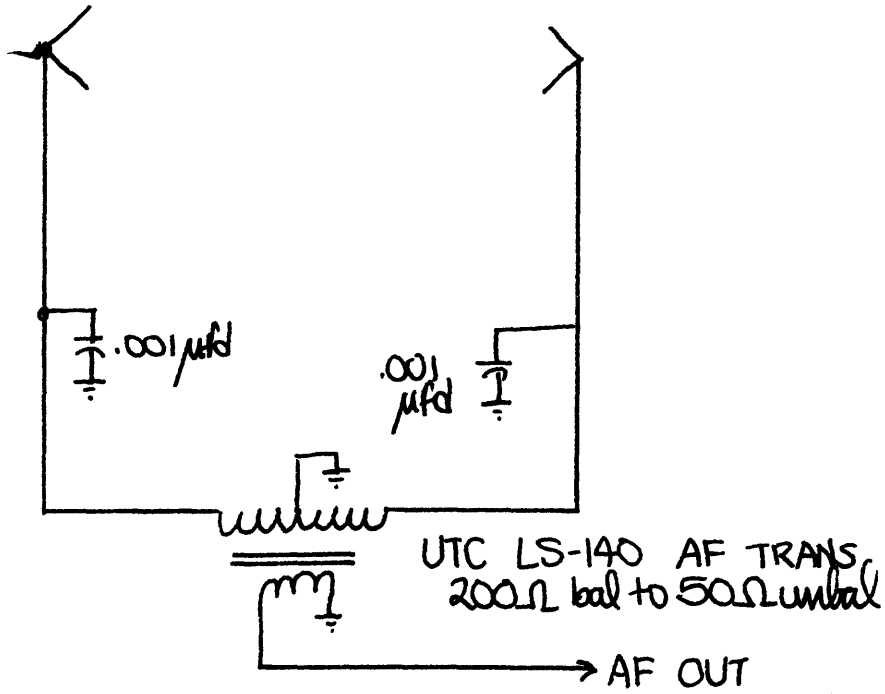

frequency through the .001 microfarad capacitors; the AF output is taken through a UTC LS-140 four to one, balanced to unbalanced impedance matching transformer, performing the same function as the hybrid transmission-line transformers at RF. The image frequency open is taken care of by the crystal filters.

No attempts were made to optimize performance, other than adjustment of LO level for lowest conversion loss, under the assumption that the same procedures should be followed as were carried out on the mixer.

## SECOND LOCAL OSCILLATOR

The local oscillator for the phase detector is crystal-controlled at a frequency of 30.000 MHz. It consists of a tuned-collector, tuned-base oscillator using a Fairchild 2N3564, feeding a class B/class C amplifier using another 2N3564, with a pi network for matching the output to 50 ohm unbalanced output impedance. The output power is +17 dbm at 50 ohms, and this is fed through a variable attenuator into the LO port of the phase detector. The phase detector internal circuitry raises the impedance level to 10,000 ohm balanced through a 4:1 plated core transformer (not a hybrid) and a 100:1 L-network, balanced, at 30 MHz. The two iron-core inductors are wound on type SF powdered-iron cores, as is the 1:1 collector tuned circuit/output transformer in the oscillator stage. The two RF chokes are "unmarked wonder" variety, showing a parallel resonance at approximately 30 MHz from internal stray capacitance. All variable capacitors are Johannsen, the 57-70 pfd. one being a 1-14 in parallel with a 56 pfd. mica capacitor. (Fig. 28)

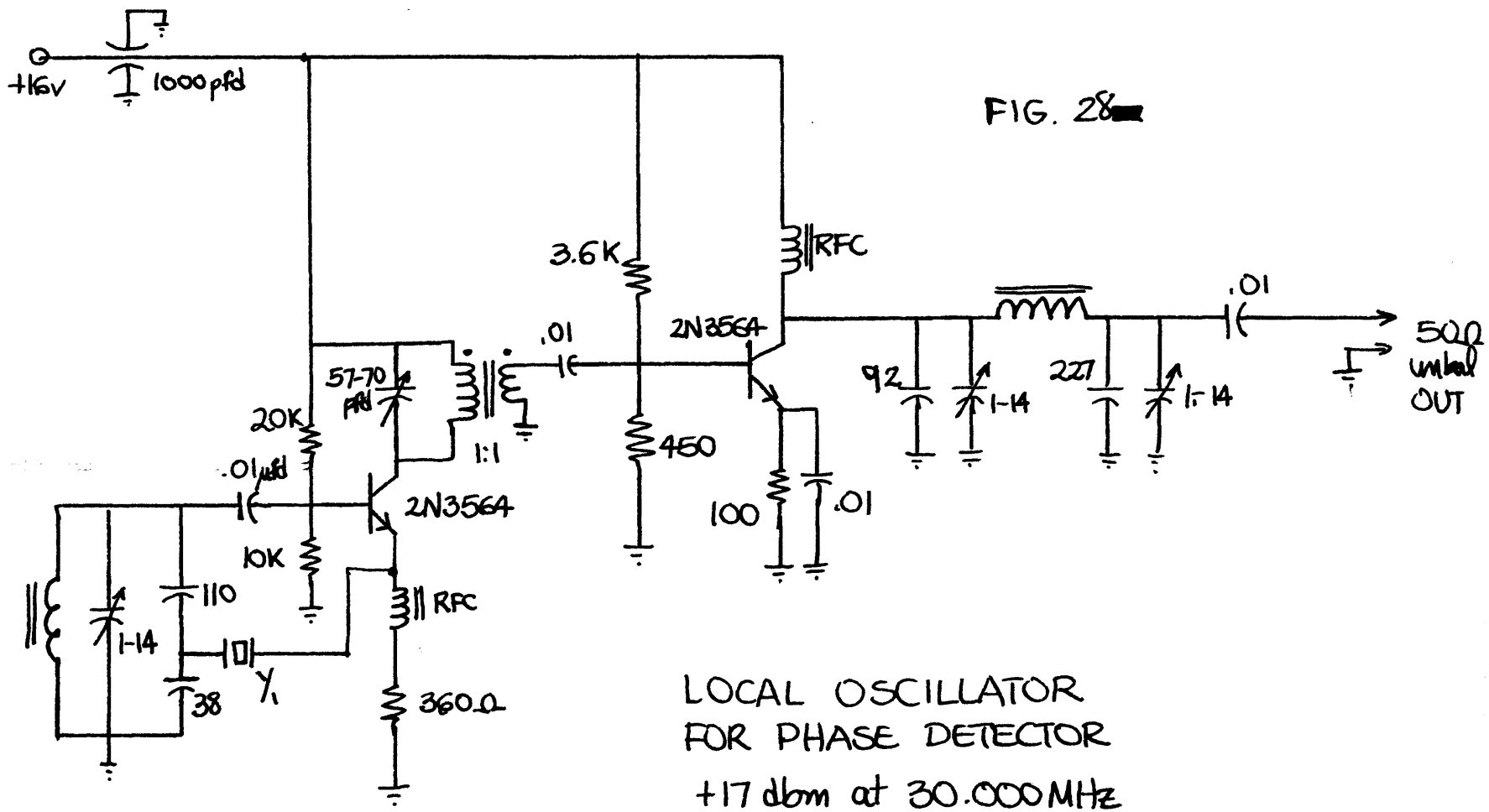


FIG. 28

LOCAL OSCILLATOR
FOR PHASE DETECTOR
+17 dbm at 30.000 MHz

$Y_1$ = 30.000 MHz
CRYSTAL

## POWER AMPLIFIER AND FIRST LOCAL OSCILLATOR

The first local oscillator is essentially a black box. The frequency is set by the Kay Model $\pi$ Sweeper, set on manual sweep; the LO signal is amplified to 2 watts average by the Power Amplifier, and fed at 50 ohms unbalanced into the LO input of the mixer.

One unfortunate limitation of this arrangement is the high shot noise level in the output of the power amplifier. The noise level is shown in Fig. 28a as measured above the system noise level; note that near the signal frequency it rises to 55 db above the noise level, and remains greater than or equal to 10 db above the noise level for 500 KHz on either side of the signal. Ordinarily this would be no problem, since the signal sensitivity is unaffected. However, if there is a strong signal near in frequency to the desired signal, it will convert the LO noise to the output frequency. If the frequency difference between the two signals is 100 KHz, the converted noise will be the power level of the undesired signal times the power level of the shot noise 100 KHz away from the LO center frequency. For example, if the undesired signal is 5 db below the level of the desired signal, and the shot noise at 100 KHz is 20 db above the noise, the noise level at the mixer output will increase by 15 db. If the desired signal is only a few db above the noise level, it will become unreadable.

The most direct solution is to use a narrower-band LO power source, one designed for minimum shot noise. This problem is not basic to the mixer, but involves instead the development of low-noise power amplifiers. Several db improvement was obtained by passing the local oscillator output through a three-cavity bandpass filter tuned to the center frequency (half-power BW of filter was approximately 500 KHz.)

FIG 28a

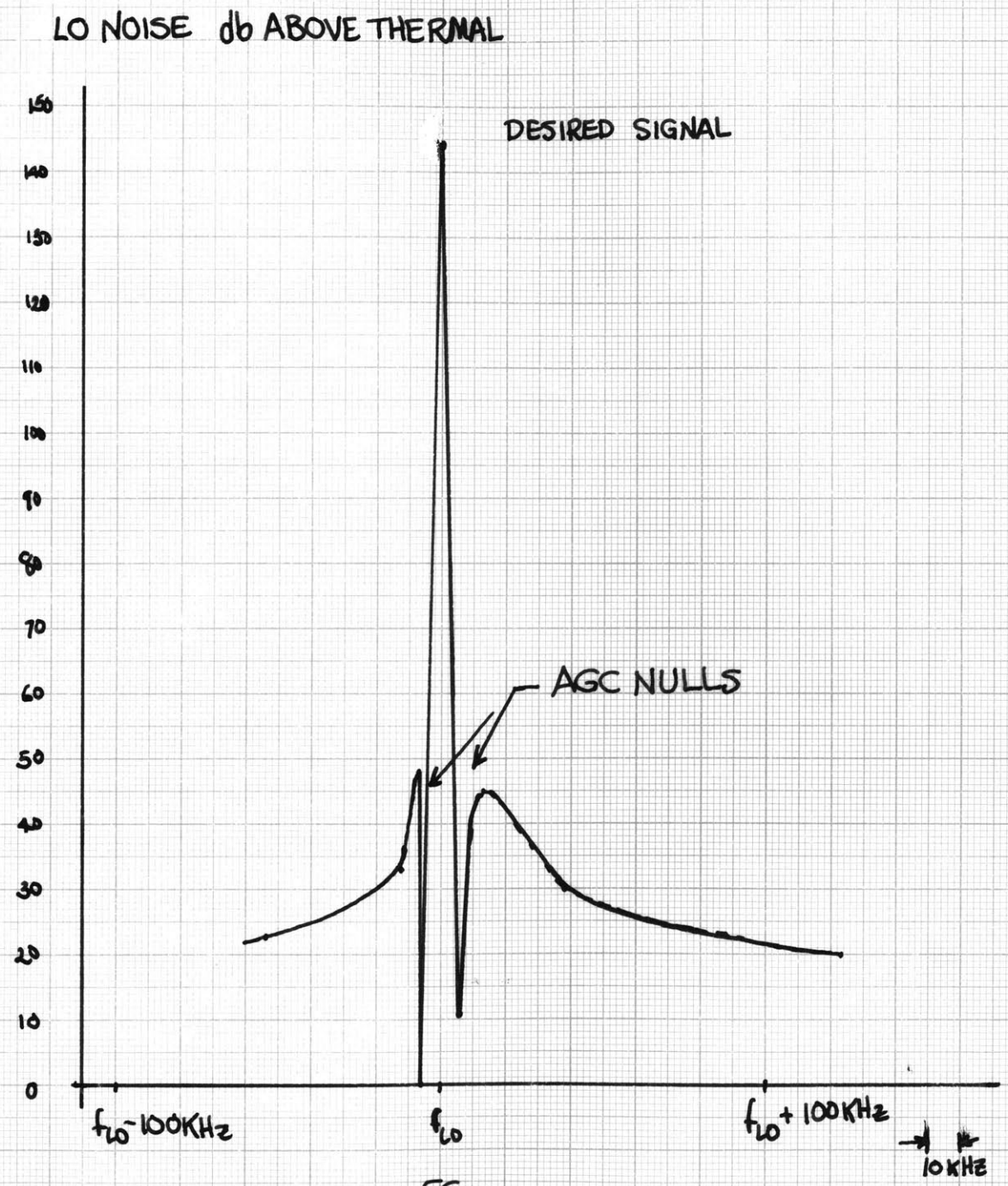
LO NOISE db ABOVE THERMAL
DESIRED SIGNAL
AGC NULLS
150
140
130
120
110
100
90
80
70
60
50
40
30
20
10
0
$f_{LO}$-100KHz
$f_{LO}$
$f_{LO}$+100KHz
10KHz

## EXPERIMENTAL RESULTS

### RECEIVER PERFORMANCE AND DYNAMIC RANGE

The experimental results of mixer/R-390 detector sensitivity and D.R. can be presented as a table, comparing them with the performance of the R-390 as a receiver operating at 10.0 MHz.

| | FET Mixer receiver | Collins R-390 |
|---|---|---|
| Sens. 10db [S+N]/N | -120 dbm | -120 dbm |
| D.R. 10db [S+N]/N | [120±5] db | 83 db |

There are several large reservations in interpreting this data; however, in a useful sense, the dynamic range of the mixer receiver is about four orders of magnitude greater than that of the Collins laboratory receiver, with the sensitivities the same. (All data was taken with a 1 KHz bandwidth in the R-390 intermediate frequency stages, used both as a detector (for the mixer) and as a receiver by itself. This set the effective noise bandwidth at 1 KHz for both systems.)

The ± 5db variation in the dynamic range measured on the mixer is not due to measurement error (which is on the order of ± 1 to 2 db on all measurements) but comes from degenerate behavior of the IM versus signal level curve for high signal levels. The physical theory of intermodulation shows that the power level of IM of the form $\cos(2\omega_i \pm \omega_j)t$ goes as the fourth power of the $I_i$ and the second power of the $I_j$; in other words, for every db increase in the power level of the signal at $\omega_i$, the IM level will increase 2 db; while for every db increase in the power level at $\omega_j$, the IM level will also increase 1 db. If both signal power levels are increased 1 db, then, the IM level will go up by 3 db. This is the Theoretical line on Fig. 29.

At high two-tone signal levels (total power at +6dbm to +14dbm) the third-order intermodulation level may stay constant with increasing two-tone power, or even decline toward a minimum point (the circle and triangle curves on Fig. 29). The exact behavior is very much a function of the FET gate bias voltages.

Although the gate DC bias voltages are made independently adjustable with the goal of matching gate turn-on characteristics, the actual voltage levels are widely different, even for separate halves of the same twin FET. One suspects, therefore, that the bias potential adjustment is matching and cancelling coefficients of the nonlinear resistance power-series expansion of the FET drain current versus drain-to-source voltage curve. It is not clear whether this operates primarily through the third-order term in direct IM production and cancellation, or through the cancellation of the second-harmonic terms at the symmetric points of the balanced bridge. In any case, adjustment of the bias potentiometers to a minimum measured IM allows a large extension of dynamic range. (In addition, nulls of varying depths occur at different potentiometer settings, lending credence to the theory that it is the cancellation of coefficients that is affected by the bias voltages. In all cases, the potentiometers are adjusted for the <u>deepest</u> IM null.) For high signal levels, the operating points of the FETs are perturbed by the signal levels, and coefficients change, moving the IM out of the gate bias null. The result is that the IM may be nulled down to an unmeasureable level at some arbitrary signal (two-tone) level, and it will increase markedly if the drive level is raised <u>or</u> <u>lowered</u>, either direction out of the null. The triangle line on Fig. 29 shows the IM behavior with the bias potentiometers set for an IM null at +9db. Although it appears that the 10 db [S+N]/N ratio line now intersects the curve at +9.5 db

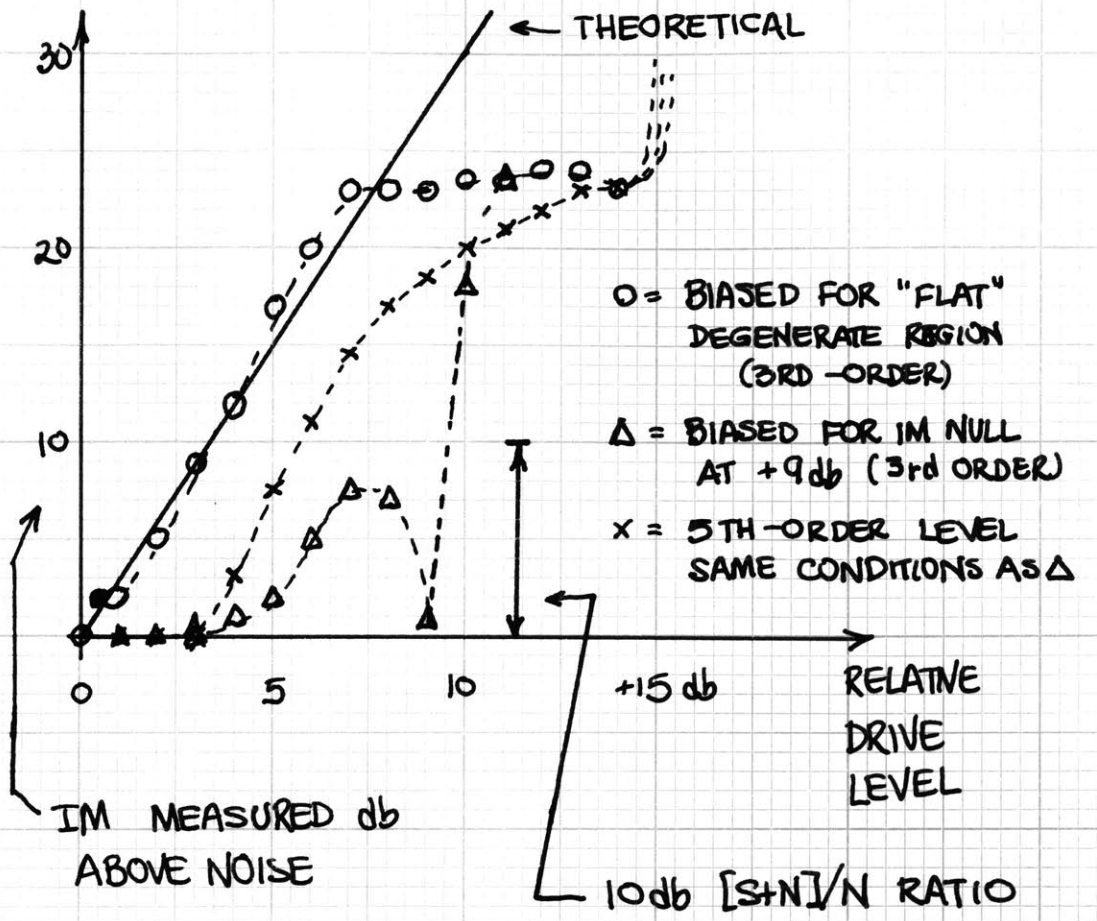


FIG. 29 IM LEVELS (3rd AND 5th ORDER) AS A FUNCTION OF DRIVE LEVEL, WITH HIGH-LEVEL DEGENERATE BEHAVIOR

instead of the theoretical value of +3.3 db, for a gain in dynamic range of 6.2 db, the fifth-order IM products (shown as the 'x' line) are now well above the third-order products. This is an unusual situation; generally the dynamic range of a mixer is so small that the fifth-order products are unmeasureable for normal two-tone power levels. The intermodulation level is now set by the amplitude of the fifth-order products, at +5.7 db, for a gain in dynamic range of 2.4 db over theoretical. As the third-order products move to the left on the graph of Fig. 29, the fifth-order curve will move to the right, and by biasing for a null at 10 to 12 db relative, the two lines may be made to cross at the 10 db [S+N]/N line, giving a dynamic range somewhere between 2.4 and 6.2 db above theoretical. The third-order IM is re-established as the point where the hump to the left of the null point crosses the 10 db line, and the actual advantage in dynamic range approaches 3 db. The greatest gain in dynamic range is possible if the flat region of the IM curve can be made to coincide with the 10 db signal plus noise to noise ratio line; in this case it is impossible, and attempts to move the flat region down end up with sharp nulls at some power level, similar to the triangle curve.

The maximum value of D.R. shown in the table, 125 db, was measured with the coefficient cancellation adjusted for maximum dynamic range; the lower value of 115 db is the value for D.R. measured with a well-behaved IM vs. two-tone level curve. The value of 125 db is usuable as a measure of D.R. in any case, since the IM level is set to remain less than or equal to 10 db above the noise level over the range 115-125 db. That is, although the IM generation process is not well-behaved, the IM level is 125 db or more below the signal level for sensitivity defined in the usual way.

The maximum dynamic range was found to occur with an LO voltage of

approximately 10.5 V RMS. At this voltage both ends of the D.R. are maximized; sensitivity peaks and the IM level nulls (not to be confused with the null found by adjustment of the FET gate DC bias level.) The gate turn-on voltage of an FET is on the order of 5.5 volts; this value of 10.5 volts RMS AC on the DC bias voltage of several volts is seen to be about the required voltage swing for optimum switching into the on and off states.

The second-harmonic behavior of the mixer (the even-order terms in the center taps of the input and output transformers, Fig. 12) is not well understood. It is expected that grounding the center taps of these transformers will provide maximum D.R., by setting the second-harmonic currents to ground and the voltages to nearly zero at these terminals. However, the best performance was found with the input center tap grounded and the output center tap open-circuited or DC grounded through a ferrite RF choke (two loops of No.26 Formvar wire through a double-holed ferrite bead, with $R_{diss.}$ approximately 1000 ohms at 30 MHz). More study is needed before the second-harmonic behavior can be completely characterized.

It was found that at the typical two-tone input levels (from 0 dbm to +15 dbm) the ferrite toroids in the original input hybrid were being driven nonlinear and generating IM themselves. This was cut down by doubling the area of the ferrite cross-section and increasing the number of turns, to cut down the internal B field and keep the core from saturating. The conversion loss of the mixer appeared to reduce the two-tone levels sufficiently that this preventive measure was not needed at the output port.

## SENSITIVITY AND CONVERSION LOSS

The system sensitivity was measured at 142 db below a +22 dbm signal, for a sensitivity of -120 dbm for a 10 db signal plus noise to noise ratio.

The thermal noise level is -204 dbW/Hz = -174 dbm/Hz = -144 dbm/ 1 KHz, for a 1 KHz bandwidth and noise bandwidth. The system sensitivity is -120 dbm for a 10 db [S+N]/N or noise level of -130 dbm. The system noise figure is

144 - 130 = 14 db.

The NF of the IF amplifier is less than or equal to 1.0 db, and the insertion loss of the rebuilt crystal filter in-band is approximately 5 db. The conversion loss of the mixer is then 14 - 1.0 - 5 db = 8 db. (There is also the additional--small--insertion loss of the low-pass filter).

According to the data sheet on the Fairchild 2N4067, the channel resistance in the fully on state is on the order of 100 to 300 ohms. Substituting this value for the $Z_{on}$ in the conversion loss expression, Eq. (46), and letting the $R_L = R_g = 200$ ohms, the transducer loss (since that is what we are actually measuring) is on the order of 7 db (for $Z_{on} = 100$ ohms) to 12 db (for $Z_{on} = 300$ ohms). It is clear that the major portion of the transducer loss comes from the channel on resistances; in addition, the load resistance is not matched, but is fixed by the 4:1 hybrid, and there is some impedance mismatch loss (included in the transducer loss formula.)

## INTERMODULATION GENERATED IN ODD-ORDER OFF-STATE REVERSE TRANSCONDUCTANCES

It is found from theoretical considerations that the off-state parasitic capacitance provides the fundamental limit in a diode mixer, generating IM at levels typically 60 db below the signal sensitivity level. While it is possible to derive the polynomial coefficients for the diode capacitance as the Taylor series coefficients of an expansion of the incremental capacitance as a function of the diode voltage around some fixed value (such as V = Ø), the physical mechanisms of the FET allow only second-order effects for cubic

and higher terms in a power series expansion of the drain to source capacitance. To estimate the effects of the higher-order terms in the $C_{ds}$ polynomial with the FET in the off state, the incremental capacitance was measured as a function of $V_{ds}$ on the Boonton capacitance bridge. This measures $c_{inc.}$ as the partial of charge with respect to the partial of voltage at some $C_o$ and bias voltage $V_o$. The points of $\frac{q}{v}$ are operated upon by the method of divided differences to obtain a polynomial expression for the incremental capacitance as a function of $V_{DC}$.

If $\frac{q}{v} = a + bV + cV^2 + dV^3 + \cdots$ (47)

and total capacitance (the desired capacitance) can be written as a polynomial expansion around V = 0,

$$C(V) = C_o + C_1V + C_2V^2 + \cdots \quad (48)$$

then all the $C_i$ are constants and we can write $Q(V) = VC(V)$ (49)

and $\frac{q}{v} = \frac{Q(V)}{V} = C_o + 2C_1V + 3C_2V^2 + \cdots$ (50)

hence $C_o = a$, $C_1 = b/2$, $C_3 = c/3$ etc. and we have a complete expression for the total capacitance as a function of the DC bias voltage over some range near V = 0. The current through the channel is then $\frac{d[Q(V)]}{dt}$ and the current (intermodulation)is then equal to

$\frac{d}{dt}[C_2V^3]$ where V is the total instantaneous voltage across the drain to source. If $V = V_i\cos\omega_i t + V_j\cos\omega_j t$ for third-order IM with $2\omega_i-\omega_j = \omega_{sig}$ then the intermodulation current is

$$I_{IM} = \frac{d}{dt}[C_2(3/4)V_i^2V_j\cos(2\omega_i-\omega_j)t] \quad (51)$$

$$= -\frac{3}{4}C_2V_i^2V_j[\ (2\omega_i-\omega_j)\sin(2\omega_i-\omega_j)t\ ] \quad (52)$$

where $2\omega_i-\omega_j = \omega_s$ and if we let the i and j frequencies have equal amplitudes

$$V_i = V_j = V \tag{53}$$

the intermodulation current amplitude is $\frac{3}{4}C_2V^3\omega_s$ .

If the parasitic impedance is on the input across the input port (as in Fig. 11) the voltage across it is approximately the same as the voltage across the load resistor (Fig. 30) and

$$V = \frac{V_{IN}R_{IN}}{R_{IN}+R_g} \tag{54}$$

The signal current in the load resistor (here designated $R_{IN}$, the input resistance of the mixer from the load resistance transformed bilaterally) is approximately

$$I_{IN} = \frac{V_{IN}}{R_g+R_{IN}} \tag{55}$$

$$\text{Dynamic range} = \frac{|I_{IN}|^2}{|I_{IM}|^2} = \frac{\left|(V_{IN})/(R_g+R_{IN})\right|^2}{\left|\frac{3}{4}C_2\left(\frac{V_{IN}R_{IN}}{R_{IN}+R_g}\right)^3\omega_s\right|^2} \tag{56}$$

$$\text{D. R.} = \frac{16}{9}\,\frac{(R_g+R_{IN})^4}{C_2^2V_{IN}^4R_{IN}^6\omega_s^2} \tag{57}$$

If matched, $R_{IN} = R_g$ and

$$\text{D.R.} = \frac{256}{9}\,\frac{1}{C_2^2\,\omega_s^2\,V_{IN}^4\,R_g^2} \tag{58}$$

From the divided difference analysis of the incremental capacitance, the total capacitance as a function of voltage has approximately the coefficients

$$C(V) = 1.28 + 0.0051V + 0.0010V^2 + 0.0019V^3 + 0.0007V^4 \text{ pfd.} \tag{59}$$

with the error terms unfortunately large because of two-place accuracy in measurement of V on the Capacitance bridge (that is, the coefficients require more decimal places to appear than the experiment is accurate.) Nevertheless, the term

$$C_2 = 10^{-15}\ F/V^2 \tag{60}$$

over the range $-1\text{Volt} \leq V_{IN} \leq +1\text{Volt}$.

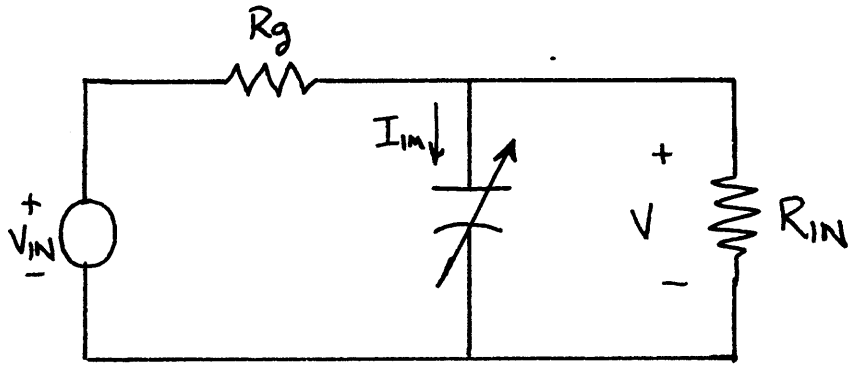


FIG. 30

CIRCUIT FOR VARACTOR IM CALCULATION

For a typical single signal input power of +3 dbm = $2 \times 10^{-3}$ Watt at 200 ohms

$$\frac{V^2_{IN(peak)}}{2(200)} = 2 \times 10^{-3} \qquad \text{and} \quad V^2_{IN} = 8 \times 10^{-3} \times 10^2 = 0.8$$

$$V^4_{IN} = 0.64$$

$$\text{D. R.} = \frac{256}{9} \frac{1}{(10^{-30})(4\pi^2 \times 10^{14})(0.64)(4 \times 10^4)} \tag{61}$$

$$\text{D. R.} = \frac{1}{(9)(40)(10^{-14})} = 2.8 \times 10^{11} = 114.5 \text{ db} \tag{62}$$

with the addition of 3 db because of equal individual powers in the two-tone

D. R. = 117.5 db.

Inasmuch as the values for $C_2$ make the final answer accuracy $\pm$ 15 db, the actual value is within the limits of the measurement arror of the calculated value.

It appears, then, the fundamental limit on the dynamic range of an FET operating as a mixer with the signal at the source is the incremental source-to-drain capacitance. The experimental mixer is operating at or near this dynamic range. If we are careful and take the undesired signal voltages at the power levels at which the output IM is exactly 10 db above the noise level, the value calculated should be exactly the same as the experimental value. For [illegible] two-tone at +3 dbm (each power) the approximate level at which this much IM output power is generated, the calculated value is within the limits of the experimental identical to the measured value for dynamic range.

# CONCLUSIONS

An unusual mixer using four field-effect transistors in a balanced-bridge configuration has been analyzed in terms of both ideal models and approximate representations of the departures from the ideal case. The two limits on dynamic range, system sensitivity and intermodulation levels, were found to depend primarily on device characteristics which can be measured as departures from the ideal device model, and the dynamic range of a mixer can be calculated from these measurements, to within a few decibels.

It is worth looking for possible improvements in dynamic range through more complete mixer characterization and better device characteristics. At the present, the effects of second-harmonic terminations in the mixer are not clearly defined, and more work is needed to describe them. It is possible that a DC bias voltage between the source and the drain of the FETs would be able to move the $C_{ds}$ onto some portion of its curve in which the $C_2$ term is zero for reasonable excursions of voltage. The FET model, which at its simplest consists of a channel resistance in series with the parallel combination of a drain-to-source capacitance and back-to-back diodes, from source to substrate and drain to substrate, indicates that better offstate capacitance behavior should result if the gate is located midway down the channel, so that the two diodes will have equal characteristics and their odd-order terms will cancel each other out, leaving only the effect of the pinch-off depletion region capacitance. With regard to sensitivity, the conversion loss of the FET mixer could be reduced if the on resistances were negligible compared to the generator and load resistances, and the load resistance were matched for maximum power transfer (or, for minimum noise figure). The insertion loss of the rebuilt crystal filter also contributes 5 db to the

system noise figure, and some more effort should be expended in trying to reduce this insertion loss. The easiest way to gain dynamic range is to increase sensitivity, since every db increase in sensitivity allows a 2 db decrease in IM level through resistive padding and signal attenuation at the input. In short, although this mixer--receiver works at the limits of the individual device characteristics, further improvements are possible.

## FOOTNOTES

1. Torrey and Whitmer, pp 111-178
2. Rafuse
3. Lange
4. Caruthers
5. Thompson
6. Rafuse, op cit
7. Ibid.
8. Torrey and Whitmer, op cit
9. Wallmark and Johnson, pp. 309-311
10. Richer and Middlebrook
11. Fitchen and Sundberg
12. Middlebrook
13. Lepoff and Cowley
14. Orloff
15. Gretsch

## BIBLIOGRAPHY


Torrey, H. C., and C. A. Whitmer, Crystal Rectifiers, McGraw-Hill, New York (1948)

Wallmark, J. T., and H. Johnson, Field Effect Transistors--Physics, Technology, Applications, Prentice Hall, New Jersey (1966)

Rafuse, R. P. "Low Noise and Dynamic Range in Symmetric Mixer Circuits" Cornell Conference on High Frequency Generation and Amplification, August 29-31, 1967, Cornell University, Ithaca, New York

Caruthers, R. S. "Copper Oxide Modulators in Carrier Telephone Systems" Bell System Technical Journal, Vol XVIII, April, 1939 pp305-337

Lange, J. H. "The Fet As A Wide Dynamic Range Mixer and Amplifier" MIT S.B. Thesis, June 1967

Thompson, K. D. "The Use of Schottky Barrier Diodes in VHF/UHF Mixer Applications" MIT S.M. Thesis, June 1966

Richer, I., and R. D. Middlebrook. "Power Law Nature of Field-Effect Transistor Experimental Characteristics" Proc. IEEE , August 1963 p. 1145

Middlebrook, R. D. "A Simple Derivation of Field-Effect Transistor Characteristics" Proc. IEEE, August 1963, p. 1146

Fitchen, F. C. and G. C. Sundberg. "Conversion Gain Null in FET Mixers" Proc. IEEE January, 1967 p. 101

Lepoff, J. H., and A. M. Cowley. "Improved Intermodulation Rejection in Mixers" IEEE Trans. on Microwave T. and T., December 1966, p.618

Orloff, L. M. "Intermodulation Analysis of a Crystal Mixer" Proc. IEEE, February 1964, p. 173

Gretsch, W. R. "The spectrum of Intermodulation Generated in a Semiconductor Diode Junction" Proc. IEEE, November 1966, p. 1528

Trammell, R. D., Jr., E. E. Donaldson, Jr., and P. T. Spence. "Mixer Interference Characteristics" Georgia Inst. of Tech., Engineering Experiment Station; prepared for U. S. Army Electronics Laboratories, Fort Monmouth, New Jersey. 1964

## APPENDIX I

## INTERMODULATION

The simplest mechanism for generation of intermodulation distortion is the third order term in a v-i relationship describing the operation of some device. As has been shown previously, this third order ($V^3$ or $I^3$) term produces voltages or currents at $\omega_i$, $\omega_j$, $3\omega_i$, $3\omega_j$ and $2\omega_i \pm \omega_j$ and $2\omega_j \pm \omega_i$. With IM defined in the normal way, with $2\omega_i \pm \omega_j = \omega_s$, the IM products must still be converted to the IF frequency by a second pass, through the square-law portion of the converter. The mixer/converter must then be modeled either as a series connection of an odd-order nonlinear impedance with the corresponding even-order impedance, or as a series connection of two nonlinear impedances, the first of which produces the IM and the second which converts the IM down to the IF frequency.

Most analyses of mixer IM generation assume that an input consisting of the LO signal and two IM-producing undesired signals will give an output at the IF frequency; however, a detailed expansion of $V_{IN}=V_{LO}\cos\omega_{LO}t + V_3\cos\omega_3 t + V_4\cos\omega_4 t$ shows that instead, the mixer produces a large number of terms corresponding to the input input frequencies taken times one, two, or three, and one, two, or three at a time, such that the total of the $\omega$ coefficients (absolute values) is either one or three.

If we now allow some feedback mechanism to return these signals to the input, a large number of frequency combinations will produce IM power at the IF, the total power being the sum of the individual contributions, with proper regard for the frequency dependencies of the feedback network and the relative phases and possible cancellations of separate terms.

Let $V_{out} = r_o I + r_1 I^2 + r_2 I^3 + \cdots\cdots$ (63)

The linear and square terms will produce the same frequency terms already examined. If it is assumed that there is no second-harmonic feedback (see App. II) the intermodulation will be generated by the cubic term,

$$V_{out(cubic)} = r_2 I^3 \tag{64}$$

Then, let

$$V_{out(cubic)} = r_2 [I_{LO}\cos\omega_{LO}t + I_3\cos\omega_3 t + I_4\cos\omega_4 t\ ]^3 \tag{65}$$

where $I_3$ and $I_4$ are some undesired signals at the third-order IM frequencies

$$2\omega_3 - \omega_4 = \omega_s \tag{66}$$

The expansion of the cube term follows

$$(a + b + c)^3 = a^3 + b^3 + c^3 + 3a^2c + 3ac^2 + 3b^2c + 3bc^2 + 3a^2b + 3ab^2 + 6abc \tag{67}$$

Letting $a = I_{LO}\cos\omega_{LO}t$, b and c similarly with $I_3$ and $I_4$,

and recalling from trigonometry $\cos^3 x = (1/4)[\cos(3x) + 3\cos x]$ (68)

and $\cos x \cos y \cos z = \frac{1}{4}[\cos(x+y+z) + \cos(x-y-z) + \cos(x+y-z) + \cos(x-y+z)]$ (69)

There are ten terms in the expansion of $V_{out}$. The first term is

$$r_2 \frac{I_{LO}^3}{4}[\cos 3\omega_{LO}t + 3\cos\omega_{LO}t] \tag{70}$$

The second and third terms are of the same form, with the interchange of $I_3$ and $\omega_3$ and $I_4$ and $\omega_4$ for $I_{LO}$ and $\omega_{LO}$.

The fourth term is of the form

$$\frac{3}{2}I_3^2 I_4 \cos\omega_4 t + \frac{3}{4}I_3^2 I_4[\cos(\omega_4 + 2\omega_3)t + \cos(\omega_4 - 2\omega_3)t] \tag{71}$$

The fifth through ninth terms are similar in form with the correct currents and frequencies inserted.

The tenth term is

$$\frac{6}{4}I_{LO}I_3I_4[\cos(\omega_{LO}+\omega_3+\omega_4)t + \cos(\omega_{LO}-\omega_3-\omega_4)t + \cos(\omega_{LO}+\omega_3-\omega_4)t + \cos(\omega_{LO}-\omega_3+\omega_4)t] \tag{72}$$

The total amplitudes at each frequency are presented in TABLE II, calculated by summing all terms at each frequency.

Since $\omega_{IF}=\omega_{LO}-\omega_s$ for third-order IM output at the IF frequency we must convert down to the frequency $\omega_{IF} = \omega_{LO} - 2\omega_3 + \omega_4$ (73)

We can obtain this frequency by adding and subtracting other frequencies to the frequency of the expansion terms in TABLE II ( the middle column of TABLE II) in a square-law device generating terms of the form $\cos(x\pm y)$. That is, before we can get any output at the IF frequency, we must add or subtract other first-order or third-order terms to the terms of the cubic expansion, the addition or subtraction taking place in a square-law characteristic.

If we assume that each frequency $\omega_k$ or $\omega_1$ resulting from the cubic term can be fed back to produce a current at the input, with feedback coefficients $K_k$ and $K_m$, then the output voltage due to a sum or difference term is

$$V_{out} = r_1 K_k K_m V_k V_m \cos(\omega_k \pm \omega_m)t \qquad (74)$$

where $V_k$ and $V_m$ are the amplitudes in the right-hand column of TABLE II.

The total amplitudes at the IF frequency for each frequency combination resulting inIF output are shown in TABLE III. The $K_k$ and $K_m$ are assumed known for each frequency combination, and are left out of the total expressions in the right-hand column of this table. The total IM voltage at the output port is then the sum of the individual powers, weighted by the individual feedback coefficients.

Third-order intermodulation is thus seen to be a highly complicated phenomenon, with a number of variables that are not always easily described. The IF frequency can be built up a large number of ways, with varying amplitudes for each combination; but all combinations require a second pass through the square-law portion of the mixer.

# TABLE II

| Sym No. | frequency | add for IF output | total amplitudes ($V_k$) |
|---|---|---|---|
| 1a | $\pm[3\omega_{LO}]t$ | $-2\omega_3+\omega_4-2\omega_{LO}$ | $\frac{1}{4} r_2 I_{LO}^3$ |
| 1b | | $-2\omega_3+\omega_4+4\omega_{LO}$ | |
| 2 | $\pm[3\omega_3]t$ | $\omega_{LO}-5\omega_3+\omega_4$ | $\frac{1}{4} r_2 I_3^3$ |
| | | $\omega_{LO}+\omega_3+\omega_4$ | |
| 3 | $\pm[3\omega_4]t$ | $\omega_{LO}-2\omega_3+2\omega_4$ | $\frac{1}{4} r_2 I_4^3$ |
| | | $\omega_{LO}-2\omega_3+4\omega_4$ | |
| 4 | $\pm[\omega_{LO}]t$ | $-2\omega_3+\omega_4$ | $r_2\left[\frac{3}{4}I_{LO}^3+\frac{3}{2}I_3^2 I_{LO}+\frac{3}{2}I_4^2 I_{LO}\right]$ |
| | | $2\omega_{LO}-2\omega_3+\omega_4$ | |
| 5 | $\pm[\omega_3]t$ | $\omega_{LO}-3\omega_3+\omega_4$ | $r_2\left[\frac{3}{4}I_3^3+\frac{3}{2}I_{LO}^2 I_3+\frac{3}{2}I_4^2 I_3\right]$ |
| | | $\omega_{LO}-\omega_3+\omega_4$ | |
| 6 | $\pm[\omega_4]t$ | $\omega_{LO}-2\omega_3$ | $r_2\left[\frac{3}{4}I_4^3+\frac{3}{2}I_3^2 I_4+\frac{3}{2}I_{LO}^2 I_4\right]$ |
| | | $\omega_{LO}-2\omega_3+2\omega_4$ | |
| 7 | $\pm[\omega_4+2\omega_3]t$ | $\omega_{LO}-4\omega_3$ | $\frac{3}{4} I_3^2 I_4 r_2$ |
| | | $\omega_{LO}+2\omega_4$ | |
| 8 | $\pm[\omega_4-2\omega_3]$ | $\omega_{LO}$ | $\frac{3}{4} I_3^2 I_4 r_2$ |
| | | $\omega_{LO}-4\omega_3+2\omega_4$ | |
| 9 | $\pm[\omega_4+2\omega_{LO}]$ | $-\omega_{LO}-2\omega_3$ | $\frac{3}{4} I_{LO}^2 I_4 r_2$ |
| | | $3\omega_{LO}+2\omega_4-2\omega_3$ | |
| 10 | $\pm[\omega_4-2\omega_{LO}]$ | $3\omega_{LO}-2\omega_3$ | $\frac{3}{4} I_{LO}^2 I_4 r_2$ |
| | | $-\omega_{LO}+2\omega_4-2\omega_3$ | |
| 11 | $\pm[\omega_{LO}+2\omega_3]$ | $-4\omega_3+\omega_4$ | $\frac{3}{4} I_3^2 I_{LO} r_2$ |
| | | $2\omega_{LO}+\omega_4$ | |
| 12 | $\pm[\omega_{LO}-2\omega_3]$ | $+\omega_4$ | $\frac{3}{4} I_3^2 I_{LO} r_2$ |
| | | $2\omega_{LO}-4\omega_3+\omega_4$ | |
| 13 | $\pm[\omega_3+2\omega_{LO}]$ | $-\omega_{LO}-3\omega_3+\omega_4$ | $\frac{3}{4} I_{LO}^2 I_3 r_2$ |
| | | $3\omega_{LO}-\omega_3+\omega_4$ | |
| 14 | $\pm[\omega_3-2\omega_{LO}]$ | $3\omega_{LO}-3\omega_3+\omega_4$ | $\frac{3}{4} I_{LO}^2 I_3 r_2$ |
| | | $-\omega_{LO}-\omega_3+\omega_4$ | |
| 15 | $\pm[\omega_3+2\omega_4]$ | $\omega_{LO}-3\omega_3-\omega_4$ | $\frac{3}{4} I_4^2 I_3 r_2$ |
| | | $\omega_{LO}-\omega_3+3\omega_4$ | |
| 16 | $\pm[\omega_3-2\omega_4]$ | $\omega_{LO}-3\omega_3+3\omega_4$ | $\frac{3}{4} I_4^2 I_3 r_2$ |
| | | $+\omega_{LO}-\omega_3-\omega_4$ | |

CONTINUED

| SYMBOL | frequency | add for $\omega_{IF}$ output | total amplitudes |
|---|---|---|---|
| 17 | $\pm[\omega_{LO}+2\omega_4]$ | $-2\omega_3-\omega_4$ | $\frac{3}{4} I_4^2 I_{LO} r_2$ |
| | | $2\omega_{LO}-2\omega_3+3\omega_4$ | |
| 18 | $\pm[\omega_{LO}-2\omega_4]$ | $-2\omega_3+3\omega_4$ | $\frac{3}{4} I_4^2 I_{LO} r_2$ |
| | | $2\omega_{LO}-2\omega_3-\omega_4$ | |
| 19 | $\pm[\omega_{LO}+\omega_3+\omega_4]$ | $-3\omega_3$ | $\frac{3}{2} r_2 \cdot I_{LO} I_3 I_4$ |
| | | $2\omega_{LO}-\omega_3+2\omega_4$ | |
| 20 | $\pm[\omega_{LO}-\omega_3-\omega_4]$ | $-\omega_3+2\omega_4$ | $\frac{3}{2} r_2 \cdot I_{LO} I_3 I_4$ |
| | | $2\omega_{LO}-3\omega_3$ | |
| 21 | $\pm[\omega_{LO}+\omega_3-\omega_4]$ | $-3\omega_3+2\omega_4$ | $\frac{3}{2} r_2 I_{LO} I_3 I_4$ |
| | | $2\omega_{LO}-\omega_3$ | |
| 22 | $\pm[\omega_{LO}-\omega_3+\omega_4]$ | $-\omega_3$ | $\frac{3}{2} r_2 I_{LO} I_3 I_4$ |
| | | $2\omega_{LO}-3\omega_3+2\omega_4$ | |

MIT Libraries
Document Services

Room 14-0551
77 Massachusetts Avenue
Cambridge, MA 02139
Ph: 617.253.2800
Email: docs@mit.edu
http://libraries.mit.edu/docs

# DISCLAIMER

**Page has been ommitted due to a pagination error by the author.**

# TABLE III

| SYMBOL | AMPLITUDE AT $\omega_{IF}$ (all times respective $K_R K_m$) |
|---|---|
| 2ⓑ | $r_1\left[\frac{1}{4}r_2 I_3^2\right]\left[\frac{3}{2}r_2 I_{LO} I_3 I_4\right]$ |
| 4ⓐ | $r_1\left[\frac{3}{4}I_{LO}^3+\frac{3}{2}I_3^2 I_{LO}+\frac{3}{2}I_4^2 I_{LO}\right]\left[r_2^2\right]\left[\frac{3}{4}I_3^2 I_4\right]$ |
| 5ⓑ | $r_1 r_2\left[\frac{3}{4}I_3^3+\frac{3}{2}I_4^2 I_3+\frac{3}{2}I_{LO}^2 I_3\right]\left[\frac{3}{2}r_2 I_{LO} I_3 I_4\right]$ |
| 6ⓐ | $r_1 r_2\left[\frac{3}{4}I_4^3+\frac{3}{2}I_3^2 I_4+\frac{3}{2}I_{LO}^2 I_4\right]\left[\frac{3}{4}r_2 I_3^2 I_{LO}\right]$ |
| 7ⓑ | $r_1\left[\frac{3}{4}r_2 I_3^2 I_4\right]\left[\frac{3}{4}r_2 I_4^2 I_{LO}\right]$ |
| 8ⓐ | $r_1\left[\frac{3}{4}I_3^2 I_4\right]\left[\frac{3}{4}I_{LO}^3+\frac{3}{2}I_4^2 I_{LO}+\frac{3}{2}I_3^2 I_{LO}\right]r_2^2$ |
| 9ⓐ | $r_1\left[\frac{3}{4}r_2 I_{LO}^2 I_4\right]\left[\frac{3}{4}r_2 I_3^2 I_{LO}\right]$ |
| 11ⓑ | $r_1\left[\frac{3}{4}r_2 I_3^2 I_{LO}\right]\left[\frac{3}{4}r_2 I_{LO}^2 I_4\right]$ |
| 12ⓐ | $r_1\left[\frac{3}{4}r_2 I_3^2 I_{LO}\right]\left[r_2\right]\left[\frac{3}{4}I_4^3+\frac{3}{2}I_3^2 I_4+\frac{3}{2}I_{LO}^2 I_4\right]$ |
| 14ⓑ | $r_1\left[\frac{3}{4}r_2 I_{LO}^2 I_3\right]\left[\frac{3}{2}r_2 I_{LO} I_3 I_4\right]$ |
| [redacted] | |
| 16ⓑ | $r_1\left[\frac{3}{4}r_2 I_4^2 I_3\right]\left[\frac{3}{2}r_2 I_{LO} I_3 I_4\right]$ |
| 17ⓐ | $r_1\left[\frac{3}{4}I_4^2 r_2 I_{LO}\right]\left[\frac{3}{4}r_2 I_3^2 I_4\right]$ |
| 19ⓐ | $r_1\left[\frac{3}{2}r_2 I_{LO} I_3 I_4\right]\left[r_2 \frac{I_3^3}{4}\right]$ |
| 20ⓐ | $r_1\left[\frac{3}{2}r_2 I_{LO} I_3 I_4\right]\left[\frac{3}{4}r_2 I_4^2 I_3\right]$ |
| 21ⓑ | $r_1\left[\frac{3}{2}r_2 I_{LO} I_3 I_4\right]\left[\frac{3}{4}r_2 I_3 I_{LO}^2\right]$ |
| 22ⓐ | $r_1\left[\frac{3}{2}r_2 I_{LO} I_3 I_4\right]\left[r_2\right]\left[\frac{3}{4}I_3^3+\frac{3}{2}I_{LO}^2 I_3+\frac{3}{2}I_4^2 I_3\right]$ |

## APPENDIX II

## INTERMODULATION IN PERFECT SQUARE-LAW DEVICES

If the intermodulation products can be assumed to pass through the mixer twice (and they must, to produce an output at the IF frequency) one suspects it is possible for them to pass through the mixer three times. This double feedback loop introduces the possibility of IM a perfect square-law device.

Suppose the second harmonic current generated by the square-law mixer characteristic is fed back to the input through some FB coefficient k. The input port now has available signals at one frequency and twice some other frequency; if these are the standard undesired IM frequencies chosen so that $2\omega_i-\omega_j = \omega_s$, then the output port will have available power at the difference frequency, generated by the square-law charastic of the mixer. The final assumption holds that this difference frequency is also allowed to feed back into the input, where it combines with the local oscillator frequency $\omega_{LO}$ to produce a signal at $\omega_{LO}-(2\omega_i-\omega_j) = \omega_{IF}$.

If care is taken with the second harmonic terminations in the mixer, the feedback coefficients will be extremely small, and the IM generated by the secondharmonic behavior will be much less than that generated by the normal third-order mechanism. Interestingly enough, the dynamic range of the experimental mixer was very much a function of the second harmonicterminations; this was probably caused by the very low level of the third-order products, allowing the output to see the effects of the three-pass, double-feedback IM.